EXAMINATION OF TRANSPORT ATPASES IN MODELS OF DISEASE

by Cassandra Patenaude

A dissertation submitted to The Johns Hopkins University in conformity with the requirements of the degree of Doctor of Philosophy

Baltimore, Maryland

September, 2014

ABSTRACT

Transport ATPases make up a family comprised of six types of transporters responsible for moving molecules including but not limited to H^+, Na^+, K^+, Ca^{2+}, Mn^{2+}, Cu^{2+} and even flipping phospholipids across membrane leaflets. These versatile pumps play a major role in setting the cell's electrochemical gradient and many members arose during gene duplications from evolutionarily related isoforms. In this study we looked at the role of secretory pathway Ca^{2+}/Mn^{2+}-ATPases in colon cancer biology. Two isoforms exist in mammalian cells however mounting evidence suggests that they may not play a compensatory role. To determine if there is a distinct contribution of SPCA1 or SPCA2 to colon cancer growth we performed a simple growth assay. We found that both shSPCA1 and shSPCA2 reduced Caco-2 growth at day three due to elevations in apoptosis.

In the second part of this study, the contribution of two isoforms of the proton pump, V-ATPase a, were examined in the context of *Candida albicans* infection. *C. albicans* thrives in the gut as a commensal but maintains the propensity to establish septicemia and may become fatal. We found that the vacuolar form of a (Vph1) was responsible for vacuolar acidification and zinc clearance. Vph1 mutation, but not secretory Stv1, diminished hyphae formation and failed to establish a systemic infection in mouse. We conclude that vacuolar acidification is critical in the establishment of infection by *C. albicans*.

To my family.

Ph.D. DISSERTATION REFEREES FOR CASSANDRA PATENAUDE

Rajini Rao, PhD., Director of Cellular and Molecular Medicine and co-advisor

Mark Donowitz, M.D., Director of Basic Research, GI Division and co-advisor

TABLE OF CONTENTS

Abstract…….....ii

Table of Contents……v

List of Figures……vi

Chapter One: Intestinal Biology – A Brief Overview……1

Chapter Two: Calcium Signaling……5

Chapter Three: Secretory Pathway Ca^{2+}/Mn^{2+}-ATPases (SPCAs)……8

Chapter Four: SPCA1 and 2 in Colon Cancer Biology……13

Chapter Five: Colon Cancer and Epithelial-Mesenchymal Transitions……26

Chapter Six: SPCA2 and TRPV6 Interact in an Overexpression Model…….....33

Chapter Seven: Intestinal Microbiota……39

Chapter Eight: Candida albicans as an Opportunistic Pathogen……41

Chapter Nine: Essential Role for Vacuolar Acidification in *Candida albicans* Virulence……...43

Bibliography……..73

Curriculum Vitae……...89

LIST OF FIGURES

Figure 1: Colorectal Cancers…….....3
Figure 2: Hits for overexpression or repression of SPCAs in colon cancer……..14
Figure 3: Product from quantitative RT-PCR reaction detecting SPCA1 and SPCA2…….15
Figure 4: HA-SPCA1 and HA-SPCA2 colocalize with Golgi marker Golgin97……..15
Figure 5: Knockdown efficiencies in Caco-2……15
Figure 6: Comparing growth defects in various colon cancer cell lines……16
Figure 7: Proliferative index quantification in Caco-2……..17
Figure 8: YO-PRO-1 staining…….....19
Figure 9: Necrosis of Caco-2 lentivirally knocked down for SPCA1 or SPCA2……..20
Figure 10: Cell cycle analysis by flow cytometry of fixed Caco-2……...20
Figure 11: TER measurements in growing Caco-2 cells over time……...27
Figure 12: ZO-1 staining is intact……..29
Figure 13: E-Cadherin staining in Caco-2……29
Figure 14: Phalloidin stains f-actin at the enterocyte brush border and cortical actin……...29
Figure 15: WGA-red staining pre-permeabilizatino of polarized Caco-2……29
Figure 16: The mean surface area of Caco-2 cells……30
Figure 17: Predicted promoter eleements for human SPCA2……34
Figure 18: Fold upregulation of SPCA2 and TRPV6 in response to Vitamin D_3…….35
Figure 19: Coimmunoprecipitation of HA-SPCA1 or HA-SPCA2 with YFP-TRPV6…….37
Figure 20: NFAT translocation studies……..38
Figure 21: SPCA2 and TRPV6 are inducible in a TREx system……...38
Figure 22: Multiple sequence alignment of STV1 and VPH1 genes…….63
Figure 23: Hydrophobicity plots of CaVph1p and CaStv1p……..65
Figure 24: CaStv1p and CaVph1p localize to the secretory pathway and the vacuole, respectively……66
Figure 25: Redundant roles of CaStv1p and CaVph1p……..67
Figure 26: Isoform-specific role for CaVph1p in vacuolar acidification and zinc tolerance……68
Figure 27: Impairement of morphogenic switching in V-ATPase mutants……...69
Figure 28: Hyphal growth on solid medium is impaired in vph1 mutants……..……70
Figure 29: V-ATPase mutants have different effects on host cell infectivity in vitro……...71
Figure 30: Vph1p is required for murine systemic infection…….72
Figure 31: Validation of reintegrated VPH1……..72

INTESTIINAL BIOLOGY – A BRIEF OVERVIEW

Epithelia are responsible for establishing and maintaining a critical barrier for the host, separating self from the environment. Inherently, this cell layer must permit transport of nutrients and waste while barricading toxins and pathogens. The intestinal epithelial cell is a remarkable example of this function, separating the host from around one billion microbes per milliliter of luminal material all while facilitating rapid and efficient absorption of dietary nutrients. These cells develop a polarized cell morphology with distinct apical and basolateral membrane surfaces expressing designated transporters for water absorption, ion homeostasis, glucose transport and much more.

Under certain conditions the human intestine may lose up to one-hundred billion cells per day, and adult stem cells must replenish lost intestinal epithelial cells at an astounding rate. In addition to the growing list of intestinal stem cell populations, the gastrointestinal epithelia is comprised largely of absorptive cells (Na^+ absorptive and Cl^- secretory), as well as highly secretory cells including Paneth cells, enteroendocrine cells and goblet cells. In all models of intestinal stem cell biology, replicative cells are retained within the intestinal crypt and nonreplicative cells migrate up the crypt-villus axis toward the intestinal lumen.

Cancers of the intestinal epithelium are common with high prevalence in westernized countries. Over 100,000 individuals were newly diagnosed with colon cancer in the United States during 2013, and over 50,000 deaths from colorectal cancers are predicted for the year 2014 (NCI). A great number of lethal cancers have been prevented by routine colonoscopy. In current medical practice, all cancerous and precancerous lesions discovered must be completely removed for pathological examination. Upon histological

assessment the tumor grade, and hence prognosis, can be defined (Hassan et al. 2011, Winawer et al. 1993).

Colorectal cancer is said to begin first as a benign adenoma in the form of a polyp. This finger-like projection is ultimately caused by mutations leading to dysplasia (developmental anomaly). A fraction of these adenomas will acquire mutations allowing a subset of cells to progress toward stages of carcinoma. Alternatively, some colorectal cancers are said to develop *de novo* and may be associated with growths that have high microsatellite instability (Hassan et al. 2011).

In the 1980's it was first recognized that colon cancers arise from a single mutated clonal stem cell. Typically these epithelial stem cells must carry mutations in four or five oncogenes or tumor suppressors in order to establish a carcinoma (Ponder and Wilkinson, 1986, Fearon and Vogelstein, 1990). For example, approximately 50% of large adenomas and carcinomas carry a mutation in *kras*. Allelic loss of tumor suppressor *p53* occurs in 75% of colon carcinomas and loss of heterozygosity of *DCC* in 70% of carcinomas (Fearon and Vogelstein, 1990). In theory these mutations are acquired randomly and are selected for a growth advantage over time, behaving in a cumulative manner. Figure 1 summarizes current knowledge of mutations associated with colorectal cancer and stage.

In the mouse small intestine alone, three-hundred million cells are replaced daily to compensate for cell loss at villus tips, however, nearly all digestive cancers arise in the colon (Barker 2014). Factors that may contribute to the fifty-fold higher incidence of colon cancer as compared to small bowel cancer include a slower rate of cell loss of the

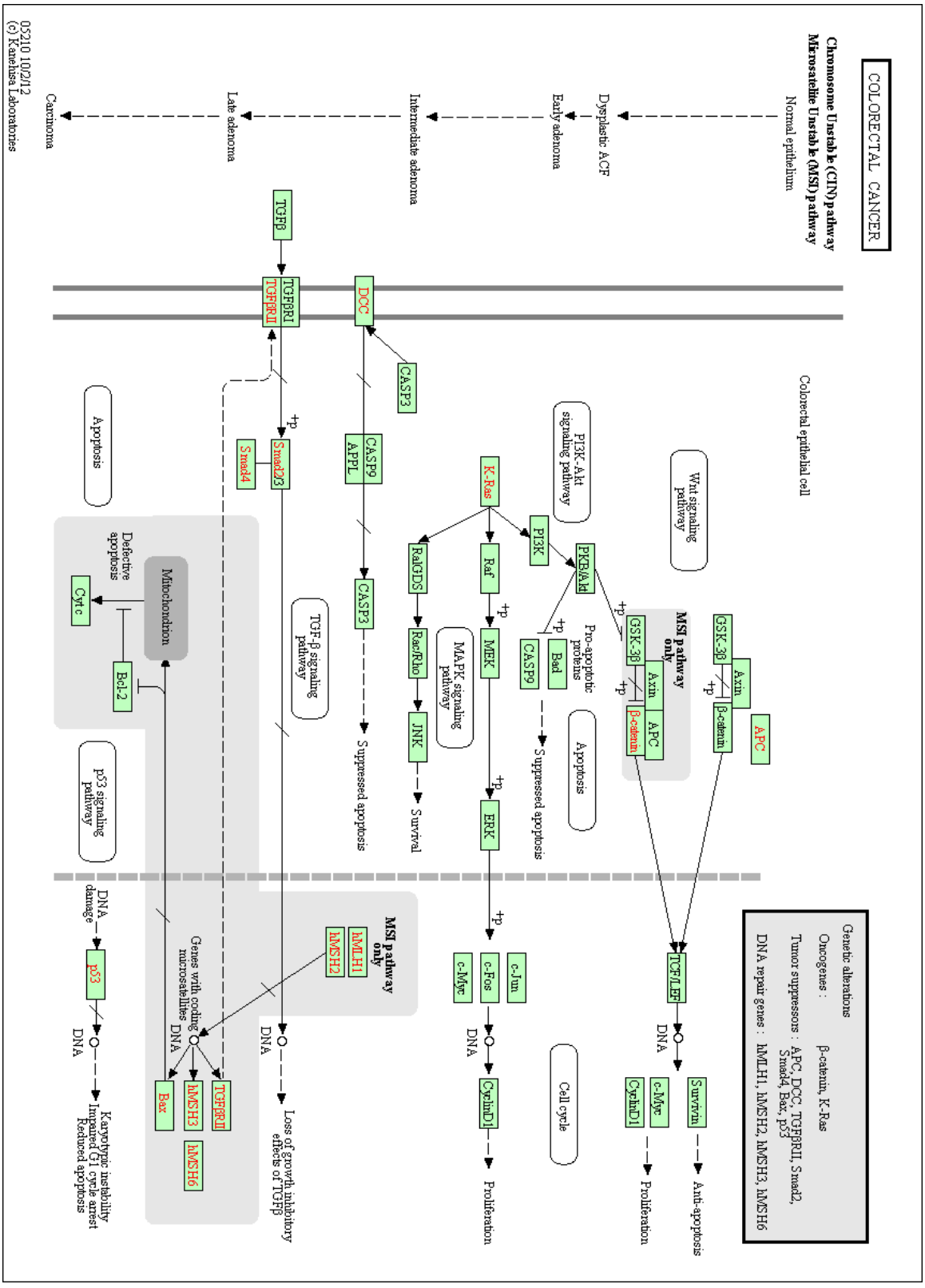

Figure 1: Common mutations in colorectal cancer appear in red text.

colon epithelium as well as a higher presence of bacteria and longer contact with stool, which may cause stress (Neugut et al. 2001). It has also been observed that apoptosis is activated in the crypt base of the small intestine but not the colon, another potential means for mutation retention in the colon epithelium (Grossmann et al., 2002). As epithelial cells reach the villus or luminal surface they undergo apoptosis and subsequent shedding. Electron micrographs reveal the formation of apoptotic bodies following nuclear condensation, with apoptosis late in the crypt-villus axis when sample preparation is delayed (Hall et al. 1994). In contrast, detection of cleaved caspase-3 (a protease activated in early apoptosis) shows increasing staining at villus or luminal planes (Grossmann et al., 2002). In rare instances a cell may resist the normal sequence of events and give rise to a malignant lesion.

Conditions increasing one's risk of either small bowel or colon cancer includes FAP (familial adenomatous polyposis a hereditary mutation in APC leading to dysregulated β-catenin) HNPCC (Hereditary Nonpolyposis Colorectal Cancer a familial mutation in DNA mismatch repair) or Crohn's disease and ulcerative colitis due to chronic inflammation (Neugut et al. 2001). However, the vast majority of patients (75%) have no hereditary linkage to the disease. There are, however, environmental factors that may increase one's likelihood of developing colorectal cancer, such as smoking, consuming a westernized diet and lack of exercise. Preventative treatments are presently being explored and include dietary nutrients and calcium. (NCI www.cancer.gov; Tomeo et al. 1999).

CALCIUM SIGNALING

Dietary calcium with vitamin D_3 supplementation has been shown to reduce the incidence of cancer in a four-year randomized study (Lappe et al. 2007). Under dietary calcium restriction, renal vitamin D is synthesized and acts on enterocytes to increase calcium absorption by generating calcium transporters TRPV6, PMCA1, and NCX1 as well as calbindin D and alkaline phosphatase. Interesting, though, duodenum from mice lacking both TRPV6 and calbindin D 9k can still induce calcium absorption in response to vitamin D_3, albeit about half WT (reviewed in Centeno et al. 2009, Benn et al. 2008) Additionally, calcium uptake induced during pregnancy can occur in the absence of the vitamin D receptor in mice (Fudge and Kovacs 2010). How calcium absorption is induced under these circumstances is not understood.

Calcium is a ubiquitous ion present in all of our cells at a low level, and is reserved for the transmission of several specific cues. A series of calcium-ATPases, exchangers, channels and buffers are responsible for keeping cytosolic calcium levels around 100nM. During calcium signaling, cytosolic free calcium levels rise and trigger a number of kinases, phosphatases and transcription factors which will be the focus of this chapter.

Before entering the cell, calcium from the extracellular space can trigger signaling through the calcium receptor, CaSR. This G-protein coupled receptor is activated by calcium from the cell surface and produces indirectly (through phospholipase C β) IP_3 and DAG. IP_3 signaling is a recurrent theme utilized in the release of calcium from intracellular stores. Both the ER and the Golgi express the IP_3 receptor, a calcium channel which releases the luminal calcium upon stimulation. Therefore, IP_3 production results in an increase in cytosolic calcium which can act on several downstream components. In

combination with DAG, Ca^{2+} activates PKC to inhibit CaSR and promote differentiation (reviewed in Lamprecht and Lipkin 2003).

One way in which PKC promotes differentiation is via blocked cyclin D1 and enhanced levels of the cyclin dependent kinase inhibitors, WAF1 and KIP1. These factors act in concert to facilitate cell cycle exit and differentiation. Additionally, CaSR signaling through PKC and phosphotyrosine kinase (PTK) stimulated MAPK and subsequent ERK1/2 signaling in an overexpression model (Kifor et al. 2001, Lamprecht and Lipkin 2003).

Components of the APC signaling pathway have also been influenced in the presence of extracellular calcium lending toward a tumor suppressing scenario. β-catenin activity is reduced and E-cadherin levels are elevated. In the unstimulated cell, β-catenin is bound to APC and destined for phosphorylation and ubiquitinylation via GSK and ubiquitin ligases, respectively. Additional β-catenin is sequestered to the cell cortex by E-cadherin. However, upon Wnt signaling (or APC mutation as is frequently seen in colon cancers, Fig. 1), the destruction complex is disassembled and β-catenin can enter the nucleus. Downstream transcription factors belonging to the TCF-family activate cyclin D1, c-MYC and Survivin to promote oncogenesis (Lamprecht and Lipkin 2003).

Interestingly, cancers that are dedifferentiated do not respond to extracellular calcium. This has been correlated with a loss of CaSR expression, thus emphasizing the importance of this receptor. However, extracellular calcium can inactivate bile acids and ionized fatty acids consequently eliminating them from potentially damaging enterocytes (reviewed in Brennan et al. 2013). For these reasons, dietary calcium supplementation may decrease incidence of colorectal cancers.

IP_3 may be synthesized in response to a number of signals including increases in cytosolic Ca^{2+}, GPCRs and RTKs. In addition to IP_3, three other calcium mobilizing messengers have been identified (Berridge et al. 2003). NAADP acts on the recently identified two pore channel, which is expressed ubiquitously and localizes to acidic vesicles. cADPR opens the RYR (ryanodine receptor) and isoform 1 (RyR1) has been found to be expressed in enterocytes (Prinz and Diener 2008). And finally, sphingosine-1-phosphate can act as a second messenger acting on intracellular receptors or as a secreted ligand binding to GPCRs (Takabe et al. 2008).

After calcium stores have been released they must be replenished. The ER triggers calcium entry in a store-operated manner via the calcium sensor, STIM1. STIM1 is a transmembrane protein that binds Ca^{2+} in the ER lumen. When calcium levels are low, STIM1 oligomerizes and forms punctate clusters on the ER membrane. These membranes can place STIM1 in juxtaposition with the calcium channel Orai1 and initiate calcium entry from the extracellular space. Recently, our lab found that Orai1 can also be opened by a Golgi-resident protein (SPCA2) in a store-independent manner. The mechanism behind this gating interaction will be discussed in the next chapter.

SECRETORY PATHWAY CALCIUM-ATPASES (SPCAS)

In this study I examined the role of the secretory pathway in colon cancer biology via the calcium/manganese transporter family, SPCA (Secretory Pathway Calcium/Manganese-ATPases). Two isoforms (SPCA1 and SPCA2) exist in tetrapods and belong to the family of P-type ATPases (Pestov et al. 2012). SPCAs have homology to other Ca^{2+}-ATPases (SERCA, PMCA) with a conserved A, N and P (actuator, nucleotide-binding and phosphorylation) domain structure. Transporters belonging to the P-Type Ca^{2+}-ATPase family have a conserved 10 transmembrane helices with loops containing SERCA-like T-G-E and D-P-P-R motifs (Van Baelen et al. 2004). An EF hand motif in the N-terminus can bind calcium and modulate the enzyme's calcium affinity (Wei et al. 1999). SPCAs have less reactivity to thapsigargin (SERCA inhibitor) or vanadate/lanthanum (PMCA inhibitors) so in order to study these pumps we use primarily genetic approaches (Ton et al. 2002).

SERCA structure and function has been studied extensively and is frequently used as a basis for understanding SPCAs. Like SERCA, SPCAs complete a reversible catalytic cycle. In the first half of the enzymatic cycle, the calcium binding site of SERCA faces the cytosol. Upon binding of two calcium ions, the enzyme is primed for phosphorylation transfer from ATP to a conserved aspartic acid. Next the phospho-enzyme may switch accessibility with the calcium-containing pore now facing the vesicle lumen. Calcium ions exit the low affinity Ca^{2+}-binding site. Subsequently, the phosphate is hydrolyzed and the enzyme can return to its original state (de Meis and Vianna 1979, Dode et al. 2002). A key aspartic acid is the site for the phosphorylation reaction and, if mutagenized, results in an inactive pump. Unlike SERCA, SPCAs have specificity for both calcium and manganese

ions and transport through one, not two, pores as site I has been mutagenized (Van Baelen et al. 2004). Thus, mutation of a conserved glutamine residue (Q783;PMR1) in the pore of SPCAs creates a pump with intact specificity for Mn^{2+} but loss of a Ca^{2+} binding site (Wei et al., 2000). The SPCA1 gene has 4 transcript variants (a-d) with SPCA1a, b, and d all having a Km for Ca^{2+} around 0.2μM. SPCA1c is missing the tenth transmembrane domain and is functionally inactive (Van Baelen et al. 2004). The substrate concentration at half saturation for Ca^{2+} transport mediated by human SPCA2 hovers around 0.25μM.

Although their transport characteristics are similar, SPCA1 and SPCA2 differ in their expression profile. With a northern dot blot, the Wuytack laboratory arrayed human tissue RNAs for both SPCA1 and SPCA2. SPCA1 is expressed ubiquitously in human tissue samples while SPCA2 has a restricted expression pattern with high expression in secretory tissues. Among samples highly expressing SPCA2 were fetal and adult lung, thyroid, salivary and mammary glands, placenta, bladder, prostate, testis, trachea and high expression was observed throughout the digestive tract from the stomach to the rectum (Vanoevelan et al. 2005). Similar findings were reported in rat tissue samples by RT-PCR, with increased variability of SPCA1 transcript across tissue samples (Pestov et al. 2012).

Immunolocalization results are mixed and depend upon the cell type analyzed and the antibody used. Vanoevelan et al. found SPCA1 and 2 localizes with the Golgi marker TGN46 in human colonic epithelial cells, in accord with localization studies of the yeast orthologue PMR1. However, in WIF-B polarizing liver cells SPCA1 localizes not only to the trans-Golgi (TGN38) but to post-Golgi vesicles adjacent to the basolateral membranes (Leitch et al. 2011). Immunohistochemistry in the rat duodenum suggests that SPCA2 localizes to the plasma membrane in these cells, unlike the perinuclear organization of

GFP-tagged SPCA2 in HT-29 cells. However, this study has shortcomings; (1) the lack of a colabel for compartment designation and (2) the absence of a biochemical study to confirm exposure on the plasma membrane (Pestov et al. 2012). SPCA2 is present in rat hippocampal neurons and has a punctate vesicular distribution partially overlapping with the Golgi (Xiang et al. 2005).

In humans, the role of SPCA1 has been more comprehensively studied than that of SPCA2. Literature on SPCA1 primarily focuses on Hailey-Hailey disease, a skin disorder that results from haploinsufficiency of SPCA1 due to a dominant autosomal mutation. Not only did keratinocytes from patients have higher resting calcium, but calcium levels remained elevated compared to healthy keratinocytes under conditions of increased extracellular calcium (Hu et al., 2000). Although Golgi and ER structure were morphologically aberrant in the SPCA1 knockout mouse (Okunade et al., 2007), human haploid keratinocytes had normal ER calcium (Hu et al., 2000). Decreased calcium in intracellular stores has been observed by Fura-2 imaging during ionomycin-mediated release in human keratinocytes (Hu et al., 2000).

In the SPCA1 knockout-derived embryonic neural tube cells, Okunade et al. found significant changes in Golgi and ER ultrastructure including dilation of both Golgi and ER, increasing disorganization of the organelles and a higher number of Golgi bodies and Golgi-associated vesicles. They also recorded an increase in apoptotic index but not mitotic index, which is the likely cause of death at embryonic day 11. Also observed was an increase in the number of lipid droplets and dense granules in the cytoplasm of SPCA1 null embryos. Interestingly, SPCA1 heterozygous mice did not develop Hailey-Hailey disease

with age but instead some mice developed squamous cell tumors of the skin and esophagus (Okunade et al. 2007).

Despite these aberrations, ultrastructural examination of tight junctions, desmosomes and basolateral membrane seemed normal, suggesting that sorting mechanisms may be intact (Okunade et al. 2007). More recently the role of SPCA1 in HeLa cells has been examined by shRNA in the context of trafficking rates. In accord with findings in the knockout mouse, SPCA1 siRNA disrupts the Golgi apparatus into disorganized vesicles and caused elevated cell death. A temperature sensitive version of VSVG was tracked in SPCA1 knockdown cells. VSVG exits from the ER to the Golgi while enroute to the plasma membrane. In SPCA1 knockdown cells, VSVG was stuck in the Golgi. Intra-Golgi and plasma membrane trafficking of VSVG was also impaired (Micaroni et al. 2010).

SPCA2 is believed to have evolved from SPCA1 during a gene duplication event some time during tetrapod evolution as it is present in amphibians, reptiles, birds, platypus and mammals (Pestov et al. 2012). In 2010 Feng et al. showed that SPCA2 (secretory-P-type ATPase 2) is involved in breast cancer aggressiveness through increasing cell cycle progression via elevations in cytosolic calcium. Unexpectedly, catalytically inactive SPCA2 also modulated cytosolic calcium to the same extent as wildtype. This phenomenon is regulated by SPCA2-triggered opening of the CRAC channel, Orai1 (Feng et al. 2010). This mechanism may actually arise from SPCA2's ability to traffic Orai1 (Cross et al. 2013). In contrast to other studies in SPCA1 deficient cells, only suppression of SPCA2 in MCF-7 cells caused a growth defect and a decrease in basal calcium in the cytoplasm.

Interestingly, gene profiling comparing healthy colon tissue versus cancer failed to detect elevations in SPCA2 but elevation of SPCA1 was found in several publications (Fig. 2a,b). Colon cancers often have genome instability with loss or duplication of alleles, a possible explanation for the data showing both overexpression and repression of SPCA transcripts. How may SPCA1 be upregulated in colon cancers? In a recent article published by Micaroni and Malquori, 2013, the ASTE1 (Asteroid1, implicated in DNA repair) gene and SPCA1 gene overlap in the human genome. SPCA1 shares its 3'UTR in sense and may be coregulatory. As they reviewed, some 80% of colorectal cancers are mutated in ASTE1 and may regulate isoform expression of SPCA1. Because isoform a and b-d have very different 3' UTRs they may be regulated by distinct miRNAs.

RESULTS

Although SPCA2 has been implicated in breast cancer aggressiveness, gene profiling data show that SPCA1 is overexpressed in colon cancers (Fig. 2a). We designed several assays to look at the role of SPCAs in colon cancer growth using the differentiating cell line Caco-2, which was derived from an adenocarcinoma and expresses many of the transporters present in the intestinal epithelium (Sun et al. 20002). As these cells become confluent they undergo programmed differentiation and form polarized monolayers that develop a transepithelial electrical resistance (TER) associated with tight junction formation. In pharmaceutical research the cell line is used for transport studies to model drug delivery *in vivo*. We used Caco-2 as a model for colon cancer and assayed for an overt growth phenotype in SPCA1 or SPCA2 knockdown.

SPCA1 and SPCA2 are detectable in human duodenum undifferentiated organoid cells by RT-PCR (Fig. 3). Additionally, HA-tagged SPCAs localize to the Golgi of Caco-2 cells similar to staining described in Vanoevelan et al. 2005 (Fig. 4). To understand the role of these transport ATPases in colorectal cancer we used a lentiviral delivery system to knockdown SPCA1 and SPCA2 individually.

In order to observe the growth of colon cancer cell lines over time we assayed for cellular NADH/NADPH with the Promega CellTiter 96 Aqueous One Solution Cell Proliferation Assay kit. The colorimetric dye, MTS (3-(4,5-dimethylthiazol-2-yl)-5-(3-carboxymethoxyhenyl)-2-(4-sulfophenyl)-2H-tetrazolium), with electron coupling agent PES (phenazine ethosulfate) undergoes a redox reaction and produces a formazan compound for assay with absorbance at 490nm. The manufacturer believes that the

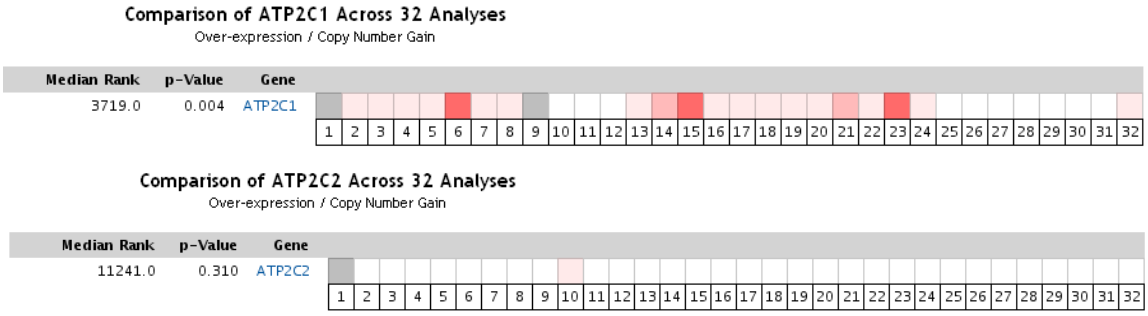

Figure 2a: Hits for overexpression of SPCAs in colon cancer as compared to healthy tissue (Oncomine). Each box represents a publication with pink-red shading indicating relative (fold or significance). Gray boxes indicate missing data.

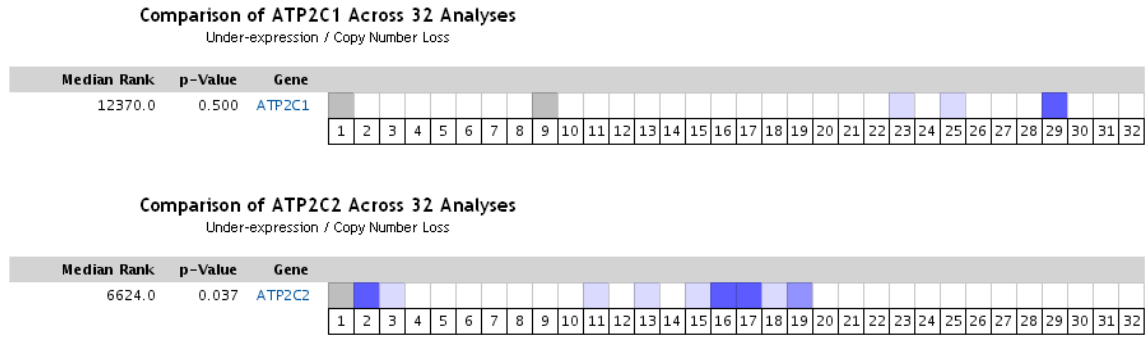

Figure 2b: Hits for repression of SPCAs in colon cancer as compared to healthy tissue (Oncomine)

compound is reduced by NADPH or NADH via cellular dehydrogenases. The change in Caco-2 cell number observed in shSPCA1 was similar to shSPCA2 and reached greater than 25% reduction by day 3. A similar growth defect has been reported in WIF-B cells for SPCA1 knockdown (Leitch et al. 2011). Additionally HCT116 had a 50% reduction in growth upon SPCA2 knockdown, but not for SPCA1. DLD1 had a reduction reaching about 30% on cell growth day 4 for only one of two hairpins tested. We next sought to identify the mechanism behind the growth changes observed due to knockdown, and predicted four possible causes comprising the proliferative, apoptotic or necrotic pathways or a delay in the cell cycle. We can find evidence for SPCAs being involved in each of these pathways/cellular processes.

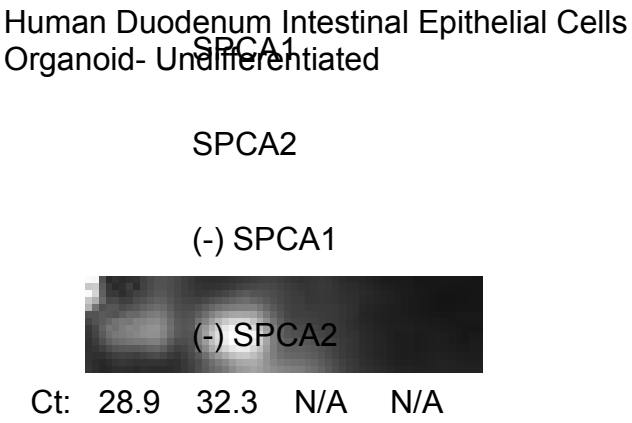

Figure 3: Product from quantitative RT-PCR reaction detecting SPCA1 and SPCA2 in human duodenum cDNA grown as undifferentiated organoids. Ct stands for cycle threshold. Primers against human GAPDH were used as a positive control.

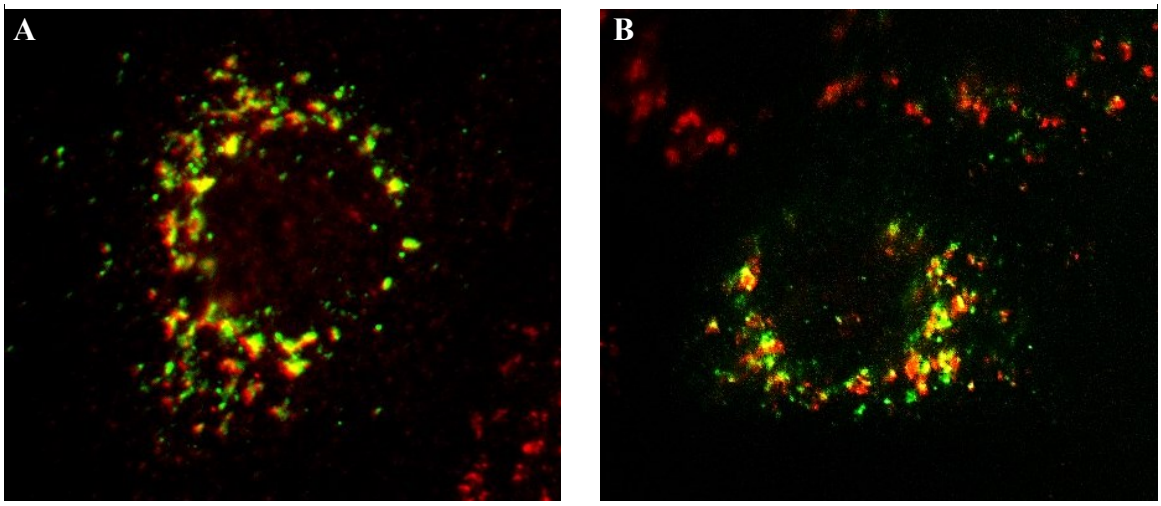

Figure 4: HA-SPCA1 (A) and HA-SPCA2 (B) (green) colocalize with Golgi marker Golgin97 (red) in transiently transfected Caco-2 cells.

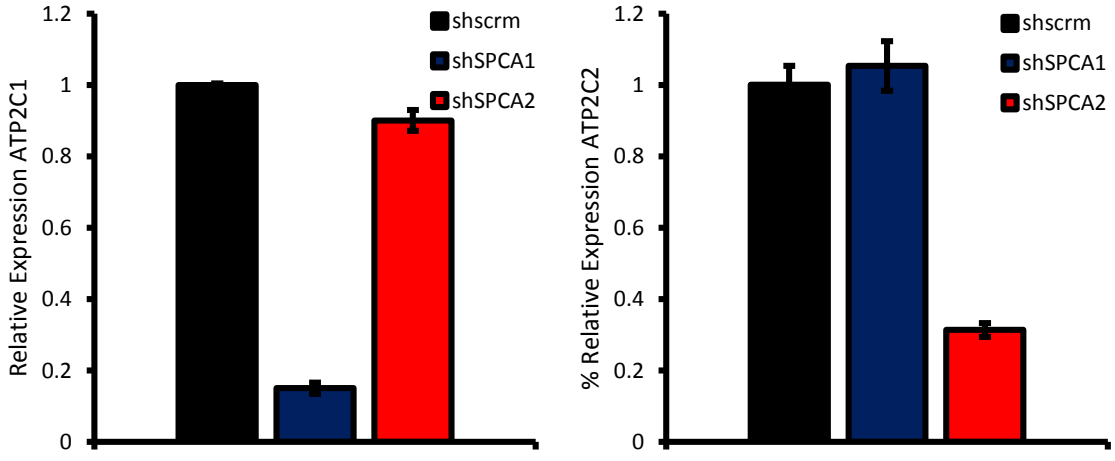

Figure 5: Knockdown efficiencies in Caco-2 were measured six days after lentiviral transduction by qPCR.

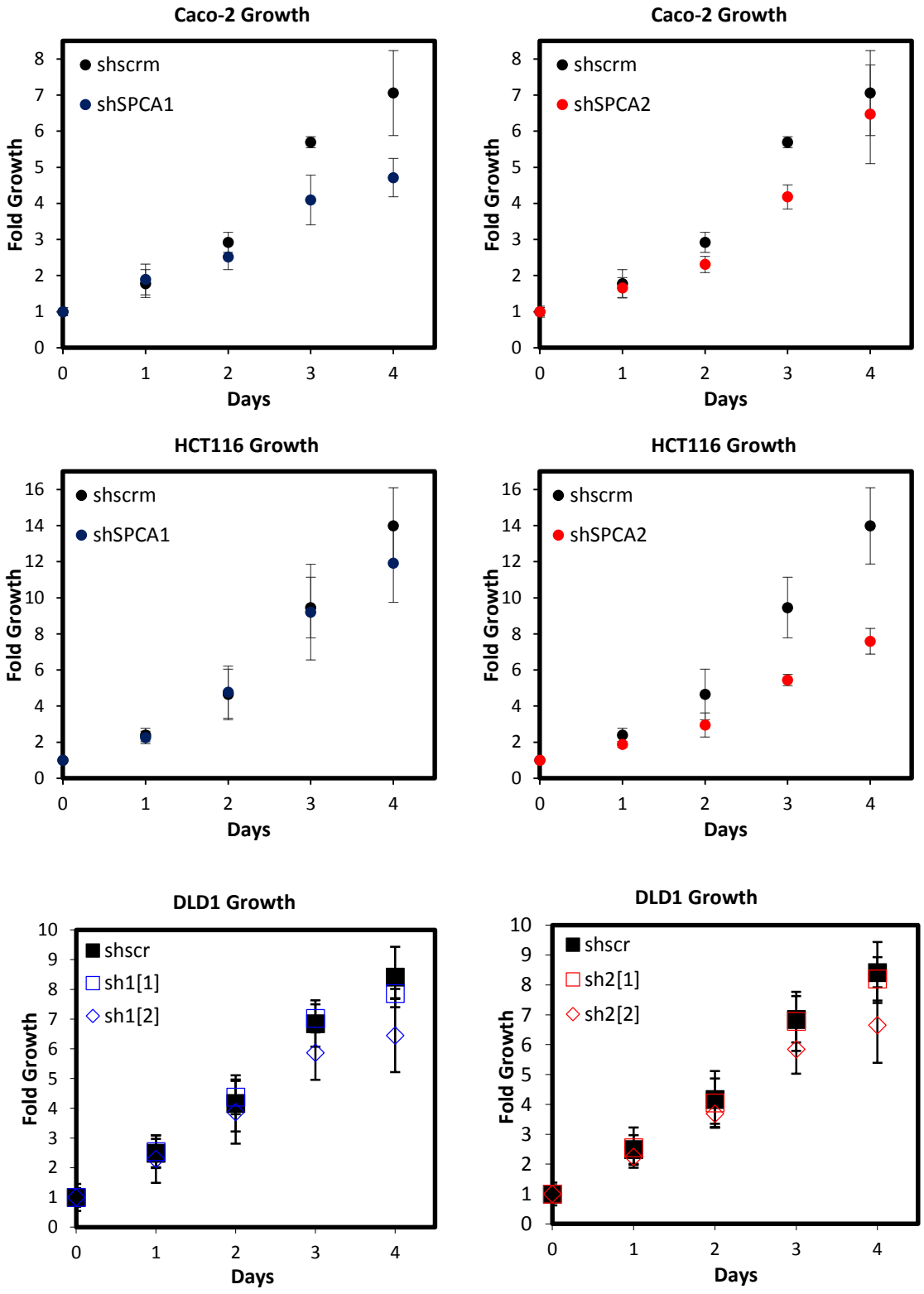

Figure 6: Comparing growth defects in various colon cancer cell lines in the presence or absence of SPCA hairpin. Error bars represent standard deviations of three biological experiments. Results from two individual hairpins were averaged for shSPCA1 and shSPCA2 treatment types.

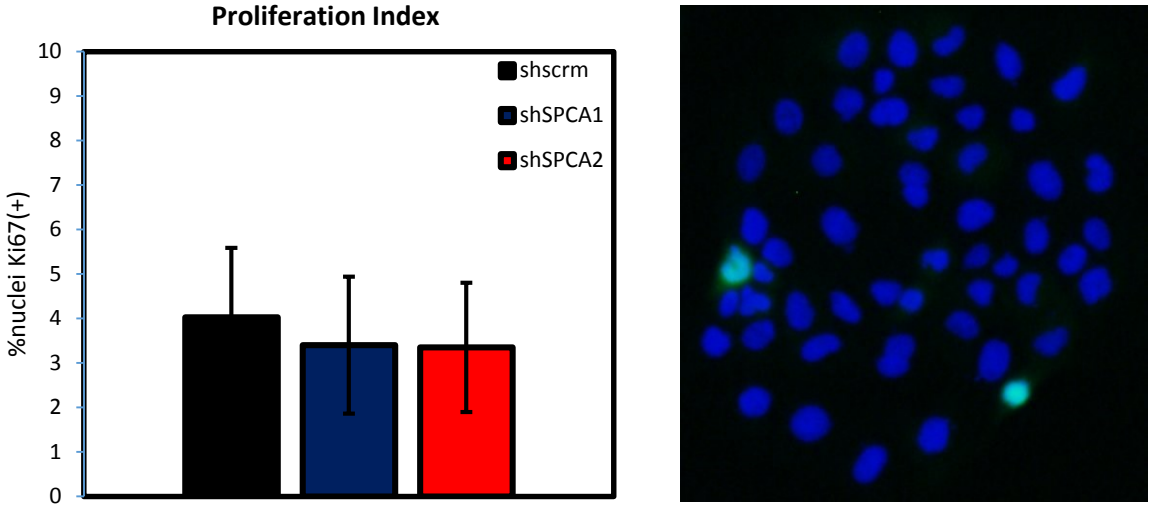

Figure 7: Proliferative index quantification in Caco-2 shows no statistically significant difference in proliferation in shSPCA treatment. Error bars represent standard deviations of three biological replicates. Immunostaining for Ki67 in control Caco-2 cells three days after seeding (right). Green staining marks Ki67 positive cells and DAPI was used to stain all cells as a control.

We assayed for cell cycle progression using antibody against Ki67, a protein that is associated with rRNA production and is expressed in all phases of the cell cycle. Its absence from G0 cells makes it suitable to quantitate the percentage of proliferating cells, also known as the proliferation index. In node-negative breast cancers Ki67 is also correlative with prognosis and sensitivity to chemotherapy (Urruticoechaea et al. 2005). Several thousand Caco-2 cells were examined at a time to calculate the percentage of cells expressing Ki67 (about 4%) and we failed to detect a statistically significant decline in proliferative index upon knockdown of SPCA. These results imply that the growth defect observed was not due to an impairment in cell cycle entry. One criticism of this assay is that only a small proportion of cells labeled positively for Ki67 and the actual proliferative pool is expected to be larger because the doubling time for this cell line is about twenty-four hours. In one report the proliferative index of primary colorectal cancers ranged from 31-99% (Michael-Robinson et al. 2001).

We looked at apoptosis by measuring cleaved caspase-3. In Caco-2 cells the mitochondrial destruction pathway is intact and can activate caspases. Staurosporine is a compound isolated from *Streptomyces staurosporesa* and is an inhibitor of numerous kinases in the cell making it a suitable positive control for apoptosis. In the nanomolar range, staurosporine inhibits CaMK-11, MLCK, PKA, PKC, and PKG and in the submicromolar range (0.2uM – 1uM) it induces apoptosis. I used staurosporine at a concentration of 2uM for 8 hrs as previously reported (Chakrabarti et al. 2003). After finding that cleaved caspase-3 was still not detectable, I treated Caco-2's with 10uM staurosporine for 24hrs (Lavaggi et al., 2011), these conditions were used for a DNA fragmentation assay which is a late event in apoptosis. At the time of protein harvest cells were visibly rounded but not detached from the cell culture surface. Cleaved caspase 3 was still undetectable.

An increase in the permeability of membranes of apoptotic cells can be detected by uptake of the selective dye YO-PRO-1. Flow cytometry of staurosporine treated Caco-2 cells revealed an increase in the uptake of YO-PRO-1 but not propidium iodide which stains dead cells. There was approximately a 50% increase in the percentage of cells that stained positive for YO-PRO-1 indicating that apoptosis was induced to some degree in shSPCAs.

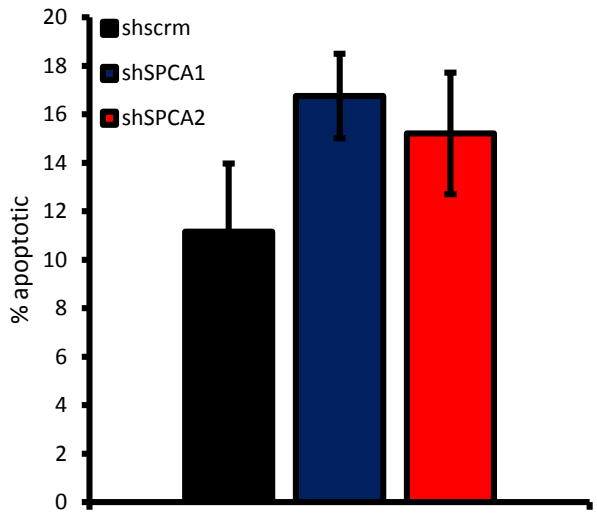

Figure 8: YO-PRO-1 staining was used to quantify the percentage of Caco-2 cells that were apoptotic upon treatment with shRNA against SPCA1 or SPCA2.

The proportion of necrotic cells was determined via assay for released LDH (lactate dehydrogenase) in cell culture supernatants. During necrosis and late in apoptosis the cell membrane loses its integrity and can leak cytoplasmic contents. Cytosolic LDH is released into the cell culture medium and can catalyze the conversion of supplemented lactate to pyruvate by utilizing NAD+ as an electron acceptor. The NADH product is next oxidized during the formation of a colored formazan product. This simple colorimetric assay revealed that only less than 1:10,000 cells were necrotic and treatment with shSPCA1 or shSPCA2 did not yield a statistically significant increase in necrosis.

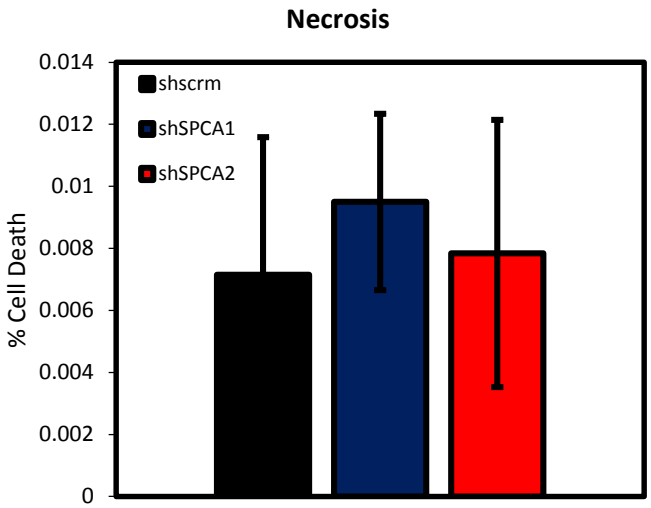

Figure 9: Necrosis of Caco-2 lentivirally knockdown for SPCA1 or SPCA2 as measured by extracellular release of lactate deydrogenase.

It is plausible that SPCA knockdown cells take longer to progress through the cell cycle. Calcium oscillations trigger transitions throughout the cell cycle. It is possible that SPCAs help to regulate this type of calcium increase. To address this, we first performed cell cycle profile analysis using propidium iodide to stain DNA. No significant change in cell cycle profile was observed upon treatment of shRNAs.

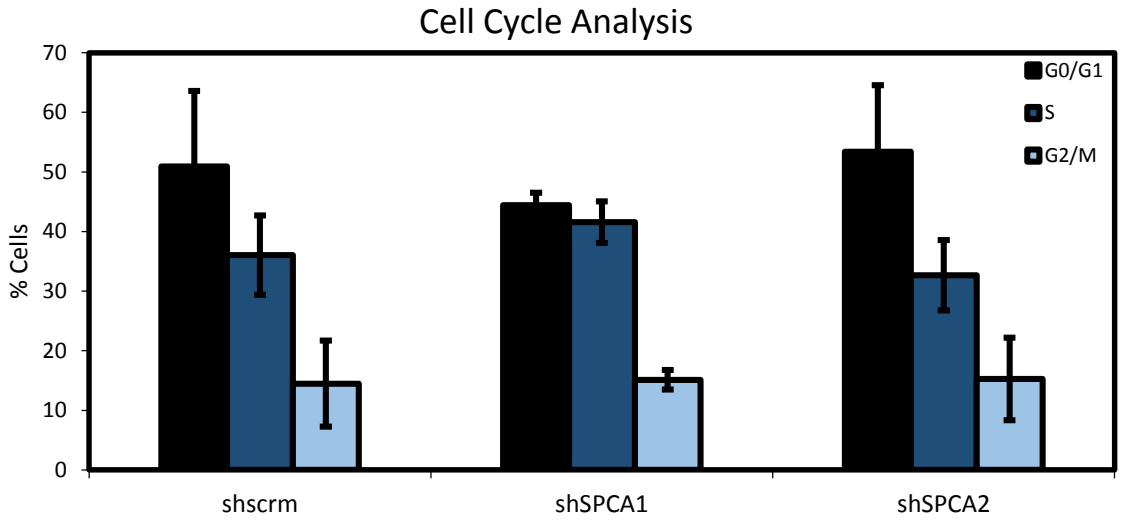

Figure 10: Cell cycle analysis by flow cytometry of fixed Caco-2 stained with propidium iodide to quantitate DNA amount.

MATERIALS AND METHODS:

Cell culture: Caco-2 bbe1 were kindly donated from the Mooseker lab (Sarker et al. 2011). Cells were cultured in DMEM with high glucose, glutamine and without sodium pyruvate

supplemented with 15mM HEPES pH 7.4 and 10% FBS. For lentiviral transduction, Caco-2's were selected under 10ug/ml puromycin for 3-7 days. Cells were deemed positive for infection if they persisted when untransduced control cells had died. Sequences used for lentivirus include (Feng et al 2010):

pLKO.1 mission (shscrm): CAACAAGATGAAGAGCACCAA

pLKO.1 509 (shSPCA1[1]): TACTTATCGTTGTTACAGTTG

pLKO.1 1016 (shSPCA1[2]): TCATCATGTTGGTTGGCTGG

pLKO.1 386 (shSPCA2[1]): GCGAACCTGTGTGGAAGAAAT

pLKO.1 1040 (shSPCA2[2]): GGAAACAACTCCTGAGTAT

Cell Growth Assay: Cell growth was monitored by the CellOne Proliferation Assay Kit (Promega). Briefly, 5e3 cells were seeded per well into a 96-well plate. Readings were taken at time 0 and consecutively every 24hrs. Cell culture media was also changed on a 24 hr basis leading up to the read date.

Cell Proliferation: Caco-2 selected for knock down were seeded at a concentration of 1e5 cells/ml onto collagen coated coverslips. Media was changed every day and on the third day cells were fixed and processed for immunofluorescent staining as previously published (Araki et al. 2003). Rabbit polyclonal antibody against human Ki67 was purchased from Santa Cruz Biotechnology (sc-15402). To determine the proliferative index, the number of Ki67 positive cells were divided by the total number of nuclei per field. Error bars represent standard deviations of the mean of three experiments.

LDH Release Assay: To assay for necrosis, cellular supernatants were collected 20 hrs after the last media change. LDH in the supernatant was normalized to total cellular LDH

and is presented as % cell death as described by the manufacturer. Samples were processed with the Cytotox 96 Assay (Promega).

Cell Cycle Analysis: Performed using propidium iodide as previously described (Riccardi and Nicoletti 2006). Briefly, Caco-2 were washed twice with HBSS, all floating cells were collected. Trypsinized cells were harvested and the reaction was stopped with addition of 5X volume of growth medium. Pelleted cells were resuspended in PBS for counting and diluting to 1e6/ml. 1 ml of cells were pelleted again and resuspended in 500ul for fixation in 4.5ml 70% ice cold ethanol. Cells were gently vortexed wile ethanol was added slowly. Fixed cells were stored at -20°C overnight before washing in PBS. Finally cells were stained in 1ml of propidium iodide staining solution (40ug propidium iodide, 50mg RNase A) for 30-60 minutes prior to analysis.

Apoptosis:

Caco-2 were harvested from the tissue culture medium and plate by trypsinization. Trypsin was inactivated with cell culture medium and pelleted cells were washed with 5ml PBS. In 1ml PBS, 1e6 cells were resuspended and 1ul each of YO-PRO-1 and propidium iodide from staining kit (Molecular Probes V13243) were added. Keep cells on ice before analysis by flow cytometry.

EdU Uptake:

To adherent cells, 20uM EdU solution was applied and cells were returned to the incubator for a 20 minute pulse. Caco-2's were harvested by trypsinization and washed in PBS with 1% BSA. Cells were stained using the manufacturer's protocol (Molecular Probes C-10424).

DISCUSSION:

Although there are multiple ways in which calcium regulates proliferation by cell cycle progression or cell cycle exit, prolonged elevations in calcium can lead to increased rates of cell death. Two overarching mechanisms of cell death are observed *in vivo*. First, apoptosis is the controlled programming of cell death in which cellular components are degraded or digested in a regulated fashion to optimize toxicity reduction. In the digestive tract epithelia are constantly replenished by the stem cell niche in the crypt; in order to counterbalance this growth apoptosis plays a major role in regulating the overall cell population, with the majority of apoptosis occurring toward the villus tip (Hall et al., 1994). Caspases are responsible for digesting intracellular proteins to prepare the cell for apoptosis, with upstream initiator caspases activating downstream effector caspases. Both intrinsic and extrinsic pathways serve to activate caspases (Reed 2000).

Alternatively, a second mechanism in which cellular components are destroyed in a dysregulated manner is termed necrosis and is the primary mechanism of cell death due to physical trauma i.e. burns and oxidative damage (Galluzzi et al. 2012). In mouse embryos lacking SPCA1, increased apoptosis was observed in embryonic neural tube cells, making necrosis a less likely cause of the hairpin-induced growth defect.

Reports of hyperoxia or DNA damage repair can delay S phase (Shenberger and Dixon, 1999; Cliby et al. 2002). As transport of Ca^{2+} and Mn^{2+} from the cytosol to the Golgi lumen is impaired in shSPCA strains, we might expect to detect an increase in levels of these ions in the cytoplasm. Manganese tends to have an antioxidant effect, complexing with small molecule metabolites to manage superoxide. In addition, Mn^{2+}-requiring superoxide dismutase of the mitochondria converts superoxide to hydrogen peroxide and oxygen, which are far less toxic. Formation of the Mn^{2+}-associated complexes seems to

require Pho80/Pho85p and Sch9p signaling and the downstream kinase, Rim15p, in yeast (Culotta and Daly, 2013).

Despite this antioxidant-promoting scenario, affected keratinocytes from Hailey-Hailey disease patients showed signs of ROS by dihydrorhodamine 123 assay (Cialfi et al. 2009). Similarly, miR-125b, activated by ROS, contributed to Hailey-Hailey disease manifestation (Manca et al. 2011). Because these keratinocytes have been removed from the host, immune responses can no longer contribute to ROS experienced by the epithelium, implying that the source of the oxidant is cell autonomous. In *Kluyveromyces lactis* yeast, elevated ROS was also observed in Δpmr1 strains and was associated with mitochondrial morphological aberrations (Uccelletti 2005). Finally, Golgi calcium signaling has been linked to mitochondrial calcium uptake in pancreatic acinar cells (Dolman and Tepikin, 2006; Dolman et al. 2005).

Growth block has been reported in Micaroni et al. 2010 (HeLa) and Leitch et al. 2011 (WIFB) as well as Okunade et al. 2007 (embryonic neural crest cells). By assessing the relative contribution of apoptosis or necrosis to shSPCA1 and shSPCA2 we conclude that the observed colorectal cancer cell growth defects are attributed to the apoptotic pathway. Attempts to detect cleaved caspase-3 failed. Cleaved caspase-3 is detectable upon treatment of Caco-2 cells with butyrate, proving that this signaling pathway is intact (Ruemmele et al. 2003). Perhaps we were unable to detect cleaved caspase-3 due to the small number of cells undergoing apoptosis on a given day (around 5%).

There are variations on cell death which were not explored in this study. In oncosis, cells swell and lose plasma membrane integrity during preparation for cell death (Majno and Joris, 1995).

In sum, both SPCA1 and SPCA2 are involved in cell survival. Given that loss of SPCA1 elevates reactive oxygen species in human keratinocytes, one could speculate that the origin of the damaging ROS is the mitochondria via impaired Golgi or ER signaling. Okunade et al. showed that Golgi and ER structure are altered in the SPCA1 knockout mouse. Alternatively, the ER monoxygenases can synthesize ROS and ultimately lead to apoptosis (Circu and Aw, 2010).

COLON CANCER AND EPITHELIAL-MESENCHYMAL TRANSITIONS

In colon cancers, the epithelial-mesenchymal differentiation axis was the first principal component and more mesenchymal-type expression profiles correlated with more advanced tumor stages (Loboda et al. 2011). Colorectal cancers are known to undergo epithelial-mesenchymal transitions during metastasis and subsequently redifferentiate at the metastatic site into epithelial cells again. This process is thought to be regulated by the tumor environment (Brabletz et al. 2005).

In the Wnt signaling pathway, Wnts bind and activate the Frizzled receptor, thus inhibiting the action of GSK3β/APC/axin/conductin complex. Under unstimulated conditions, GSK3β phosphorylates β-catenin at the N-terminus and signals the subsequent degradation of β-catenin. Conversely, GSK3β inhibition liberates cytosolic β-catenin to interact with adherens junctions or translocate to the nucleus where it exerts its transcriptional activity at oncogene promoters. Additional environmental factors play a role in β-catenin localization and action include TGFβ, TNFα, TFF3, IGFI and II, EGF and HGF. β-catenin activation causes epithelial-mesenchymal transitions or can result in failure to differentiate into epithelia (reviewed in Brabletz et al. 2005). In this system E-cadherin is a major player in β-catenin regulation.

We chose to look at what role SPCAs may be playing in Caco-2 transitioning from mesenchymal to epithelial cells. Trafficking studies in HeLa show defects in VSVG transport upon knockdown of the Ca^{2+}/Mn^{2+} ATPase, SPCA1 (Micaroni et al. 2010). Additionally, the differentiation of WIF-B cells was delayed in SPCA1 knockdown (Leitch et al. 2011). Components belonging to intracellular calcium handling have been shown to change in colon cancer progression, e.g. the loss of SERCA3 (reviewed in Lamprecht and

Lipkin 2003). We hypothesized that knockdown of SPCAs would result in trafficking defects of E-cadherin, thus altering the differentiation status of the colorectal adenocarcinoma-derived cell line, Caco-2.

Caco-2 cells induce expression of the epithelial marker protein E-cadherin in the differentiated state (data not shown), suggesting that a mesenchymal to epithelial transition may be taking place. One established measure of Caco-2 differentiation is the development of a transepithelial electrical resistance (TER). As Caco-2 mature, a tight junction forms and limits the paracellular permeability of ions across the cell monolayer. By applying a constant voltage across cells grown in cell culture inserts, a current can be recorded. TER values begin to taper around 12 days after seeding and continues to increase slightly up to day 21. We deemed day 14 cells as "differentiated" in accord with TER recordings and the literature. No delay in TER development in Caco-2 treated with shSPCA1 or shSPCA2 was found (Fig. 11). Correspondingly, immunofluorescent staining revealed that the tight junction protein ZO-1 localized correctly in control and knockdown cells suggesting that there was no developmental delay in Caco-2 differentiation upon depletion of SPCAs (Fig. 12).

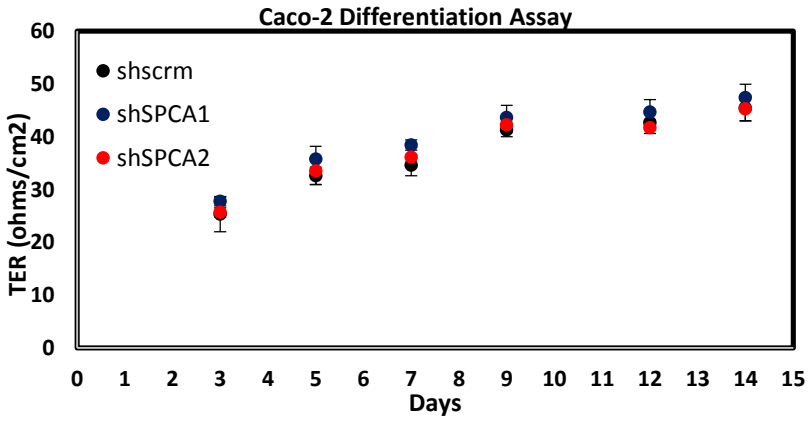

Figure 11: Transepithelial electrical resistance (TER) measurements in growing Caco-2 cells over time. As cells reach confluence they develop tight junctions and electrical resistance plateaus. No significant change in TER development was observed in SPCA knockdown. Error bars represent standard deviations of three technical replicates.

We next examined components that abide by apicobasolateral sorting pathways in polarized epithelia. E-cadherin sorting begins at the trans-Golgi network facilitated by the ARF-GEF, BIG2. A dileucine motif is essential for the basolateral sorting of E-cadherin and binds to an unknown adaptor. Vesicles carrying E-cadherin dock to Sec6/8 complexes on the lateral membranes (Bryant and Stow, 2004). Thus we performed immunostaining for the adherens junction protein, E-cadherin, which binds and sequesters β-catenin thus suppressing EMT. In HeLa, knockdown of SPCA1 resulted in missorting of the plasma membrane targeted VSVG (Micaroni et al. 2010). E-cadherin localized properly to the basolateral membranes in fully polarized monolayers, suggesting that steady state levels of E-cadherin were unaltered by shSPCA treatment.

In the late eighties and early nineties lectin staining was examined for histological differences in normal and diseased colon biopsy. We looked at wheat-germ agglutinin staining to label broadly apically localized glycosylated proteins. WGA-TRITC staining labeled the mucosa of unpermeabilized Caco-2 monolayers and seemed to have approximately the same intensity and distribution of signal. Although glycosylation defects may exist, the steady-state pool of glycoconjugates at the apical membrane appear to be the equivalent.

Phalloidin staining was performed to examine the morphology of the brush border. Phalloidin conjugated to FITC binds and labels filamentous actin in the cell, which is enriched for in the microvillus and around the cell cortex. Orthogonal sections were collected and random microvilli were selected for length calculation. The mean brush border length was the same for all three samples (3.4 – 3.7 um).

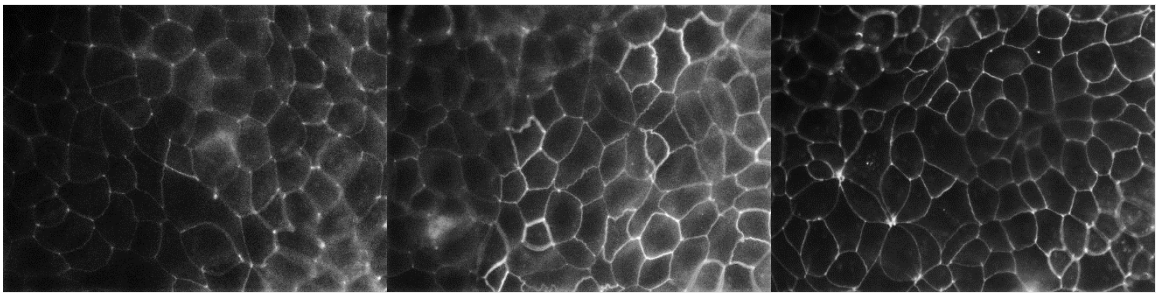

Figure 12: ZO-1 staining is intact in shscramble Caco-2 (left), shSPCA1 (center) and shSPCA2 (right) after 14 days of growth.

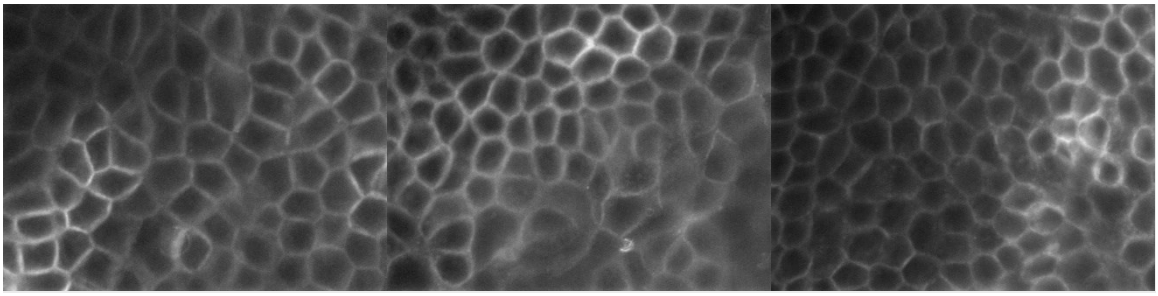

Figure 13: E-Cadherin staining in Caco-2 grown for 14 days is not altered by shSPCA1 (center) or shSPCA2 (right).

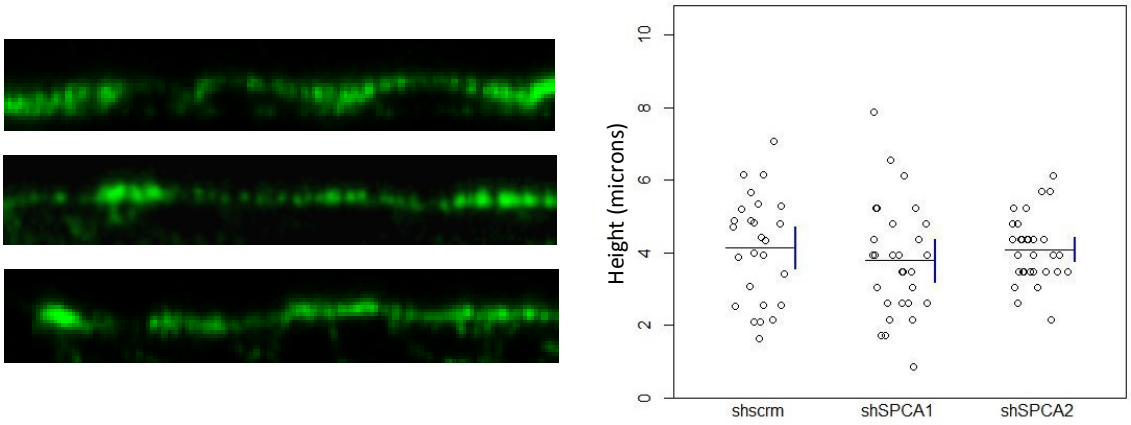

Figure 14: Phalloidin stains f-actin at the enterocyte brush border and cortical actin. On the left, a Z-stack of Caco-2 transduced with shscramble (top), shSPCA1 (middle) and shSPCA2 (bottom) exhibit normal brush border morphology. The mean brush border height was 3.4-3.7 microns (right, blue bars represent 95% confidence intervals).

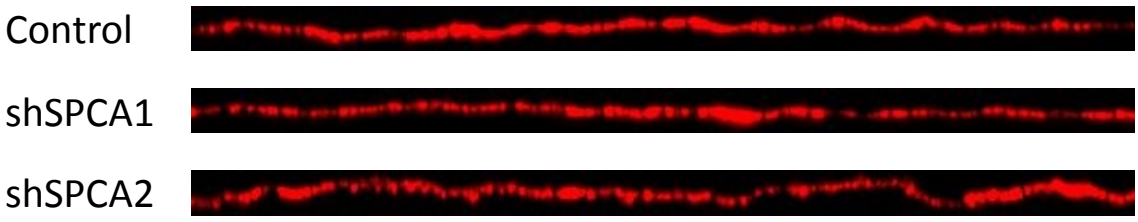

Figure 15: WGA (wheat germ agluttinin)-red staining pre-permeabilization of polarized Caco-2 cells. The mucosa appears to be equivalent in all samples.

At this time, we noticed a trend toward decreasing cell size with shSPCA2 treatment. Factors that may alter cell size and or growth rates include mTOR signaling. In Jurkat cells, prolonged inhibition of mTOR by rapamycin (inhibitor of mTORC1) had a reduced cell size and slowed growth, with more cells stuck in the G1 phase as revealed by flow cytometry of propidium stained cells at various time points. This G1 block could be reversed by the removal of mTOR inhibition (rapamycin) (Fumarola et al. 2005). However mTOR inhibition by leucine starvation blocks proliferation rather than slowing it, and subsequently stimulates apoptosis. Leucine restriction as well as LY294002 treatment did result in cell size shrinking but also increased apoptosis rates above that of control cells, implying that there may be a second signaling mechanism being altered (c-myc in leucine depletion). Of great importance, smaller cells resulting from a 24hr rapamycin treatment were resistant to drugs inducing apoptosis including staurosporine (0.3uM for 6 hrs) as revealed from DNA fragmentation and annexin-V staining for cell surface phosphotidylserine detection, and caspase 8, 9 and 3 cleavage. But is this phenomenon really due to cell size decreases or is it due to mTOR inhibition alone? Inhibition of S6K signaling was complete by 2 hours of rapamycin treatment, however at 4 hours there was no protection from apoptosis induction. On the other hand, recovery from rapamycin for 144 hours (when S6K1 phosphorylation is

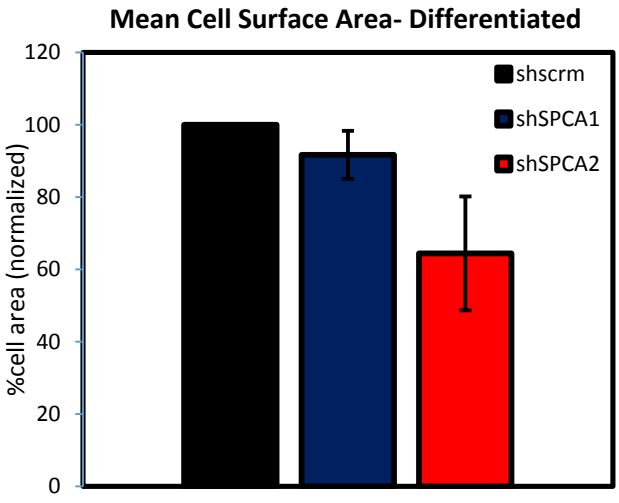

Figure 16: The mean surface area of Caco-2 cells was calculated by dividing the pixel area for a frame by the number of cells in that frame.

completely repaired), apoptosis in response to anti-CD95 antibody is restored to wildtype levels.

The SPCA orthologue, Pmr1p, has been implicated in TOR signaling in baker's yeast. *pmr1* mutant strains were less sensitive to rapamycin inhibition implying hyperactivity of TOR signaling in this background. Thus, the inhibition of TORC1 signaling was mediated by Golgi manganese levels (Devasahayam et al. 2007). Although we did not detect any evidence that the SPCAs regulate EMT in Caco-2 cells, the serendipitous observation that cell size is reduced by shSPCA2 is compelling and merits further investigation. Given that TOR signaling has been implicated in cell size regulation, the effect of SPCA knockdown on mTOR signaling deserves consideration. In addition to the aberrant ER/Golgi structures identified by Okunade et al., an increase in the number of lipid droplets in all cell types examined was found. Perhaps this is evidence that autophagy is impaired in these cells (Singh et al. 2009). Indeed, mTOR signaling inhibits autophagy (Neufeld 2012) and perhaps these nonideal metabolic conditions restrict cell size.

MATERIALS AND METHODS:

TER Measurement: Caco-2 were seeded to transwell dishes 1.5e5 cells per well. TER measurements were recorded beginning at three days post plating and values were subtracted from those obtained from a sterile well.

WGA and Phalloidin Staining: Caco-2 were allowed to differentiate for 14 days on a collagen coated coverslip. In order to stain for wheat germ agglutinin, cells were labeled with 1:100 TRITC-WGA in DMEM for 5 minutes before washing and fixing cells as

described under immunofluorescence staining. To stain for phalloidin, cells were stained with 1:100 phalloidin-FITC for 30 minutes in PBS with 1% BSA.

Immunofluorescence Staining: Immunofluorescence staining protocols were modified from Araki et al. 1993. In brief, cells were washed twice in PBS before performing a pre-extraction in 0.025% saponin in PHEM buffer (60mM PIPES, 25mM HEPES, 10mM EGTA, and 2mM $MgCl_2$ at pH 6.8) for two minutes. Cells were washed two times in saponin/PHEM buffer containing 8% sucrose. For fixation, cells were incubated in 4% paraformaldehyde in PBS plus 8% sucrose for 30 minutes in the dark. After washing blocking and staining procedures were continued in PBS plus 1% BSA with 0.025% saponin. DAKO Antifade Mounting Solution was used for final mounting of coverslips.

Mean cell surface area: Caco-2 were differentiated for 14 days after seeding transduced and selected cells. Cells were seeded at a concentration of 1.5e5 cells/ml. After 14 days, cells were stained for E-cadherin and imaged using epifluorescence. The mean area per cell was calculated by dividing the frame area in pixels^2 by the net total of Caco-2 cells within a given frame.

SPCA2 AND TRPV6 INTERACT IN AN OVEREXPRESSION MODEL

We became interested in the possibility that SPCA2 may be involved in calcium absorption through the digestive tract. The duodenum is responsible for absorbing the vast majority of calcium via the TRPV6 channel, which is said to be constitutively active. However, as mentioned above, the duodenum can exhibit increased calcium absorption in response to vitamin D even in the TRPV6 knockout (reviewed in Centeno et al. 2009, Benn et al. 2008). The Golgi apparatus is involved in calcium absorption in enterocytes and is vitamin D-responsive (Freedman et al 1977). Additionally, calcium transport in Golgi-derived vesicles from rat intestine was increased if rats were treated with vitamin D_3 prior to extraction. This transport was ATP dependent. (Arab and Ghishan 1989). Retinoid X receptors (RXRs) can dimerize with vitamin D receptors (VDR) to form a transcriptional activating unit that acts on vitamin D response elements. Nearly 500bp upstream of the SPCA2 gene a RXRA/VDR binding site can be found, thus it is plausible that isoform 2 is responsible for the hormone sensitive transport reported (Fig. 17).

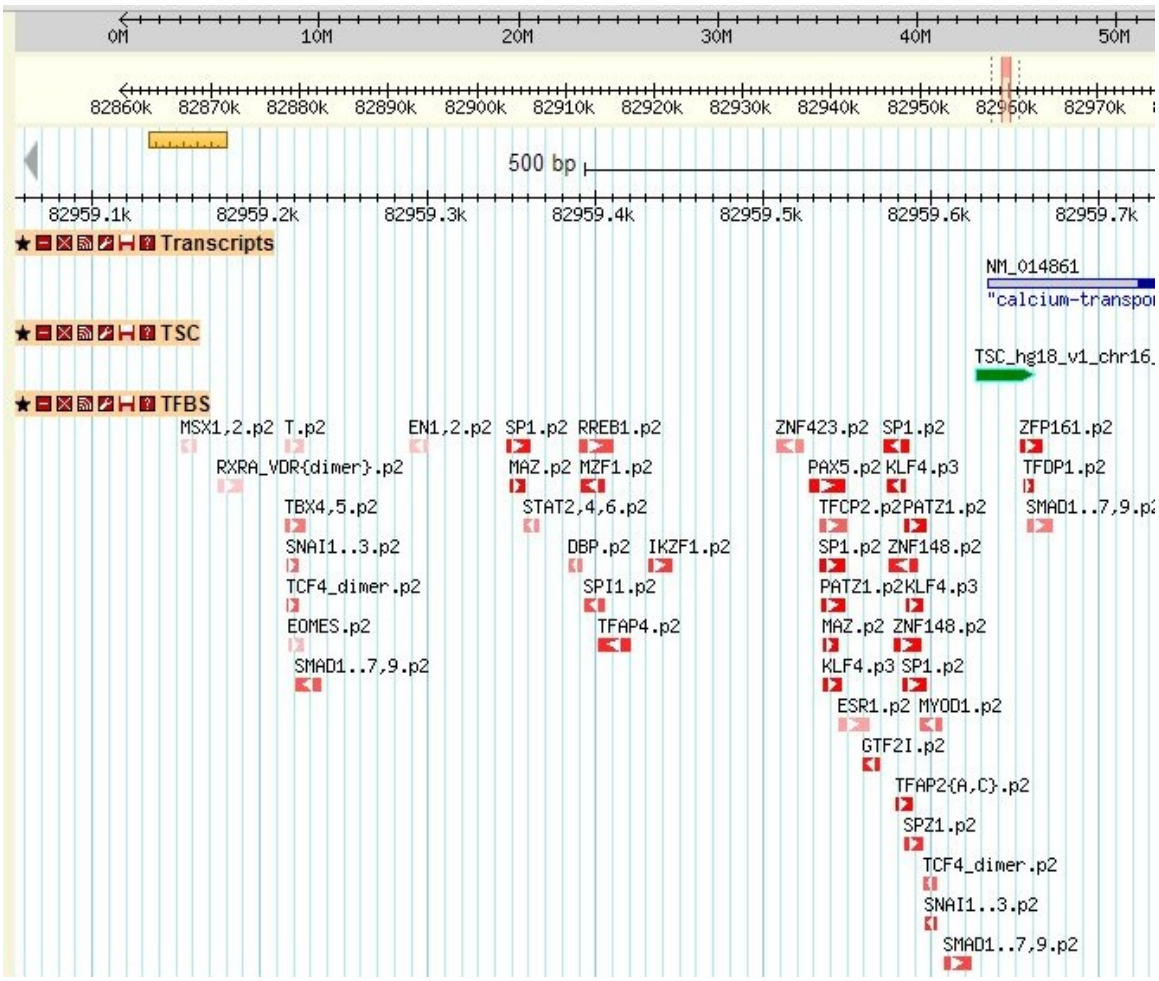

Figure 17: Predicted promoter elements for human SPCA2. SwissRegulon: a database of genome-wide annotations of regulatory sites. Mikhail Pachkov, Ionas Erb, Nacho Molina and Erik van Nimwegen. Nucleic Acids Research, 2007, Vol. 35, Database issue D127-D131.

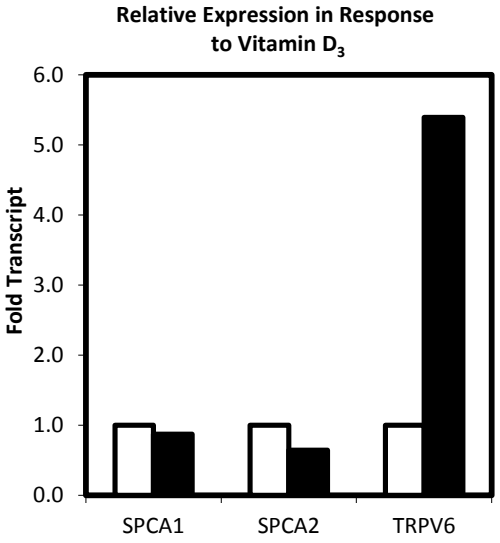

Figure 18: Fold upregulation of SPCA2 and TRPV6 in response to Vitamin D_3 treatment.

We hypothesized that SPCA2 may be responsible for this effect via store-independent calcium entry (SICE). First, we tested whether or not SPCA2 transcript was induced in response to vitamin D3 (100nM) for 24 hours. Cycle threshold values were normalized to GAPDH. Although TRPV6 transcript was induced over five-fold, we did not detect an increase in the transcript levels of either SPCA1 or SPCA2. Therefore SPCA1 and 2 are not transcriptionally regulated by vitamin D3. Fold induction of hTRPV6 is in accord with previously published studies (Fleet et al. 2002) showing a 3-fold induction upon vitamin D_3 treatment of Caco-2 bbe1.

We next sought to test whether or not SPCA2 may be involved in a calcium entry mechanism that involves the TRPV6 channel. Like Orai1, TRPV6 has been implicated in SOCE for numerous reasons. First, TRPV6 is highly selective for calcium transport. TRPV6 also shares some biochemical features of the CRAC channel (Krebs and Michalak, 2007). Additionally, preliminary data from the lab shows that SPCA2 can interact with a number of TRP channels. To this end, we hypothesized that SPCA2 interacts with TRPV6 and that this interaction regulates calcium entry through the TRPV6 channel, thus implicating SPCA2 in transepithelial calcium transport in the intestinal epithelium.

In HEK293 cells, epitope-tagged SPCA and TRPV6 were co-immunoprecipitated with antibody against HA or GFP. First SPCA2 appeared to bind TRPV6 specifically

because SPCA1 was undetectable in the pull down lane. In retrospect, this observation may be due to the reduced expression of SPCA1 compared to SPCA2 via ectopic plasmid DNA. Second, we attempted to identify the interacting domain(s) of SPCA2 by mutational analysis (Feng et al. 2010). In these constructs, SPCA2 N or C termini (or both) were swapped with the sequences for SPCA1. Pulldown with antibody against HA may have been convoluted by the nonspecific binding of YFP-TRPV6 (Mike Caterina, personal communication). To control for this, we pulled down with antibody against GFP in order to detect HA-SPCA binding. All expressed HA-SPCAs bound to YFP-TRPV6, including SPCA2 constructs in which N or C-termini involved in Orai1 interaction have been mutagenized to carry SPCA1 sequences. Thus we conclude that SPCA interactions with TRPV6 does not mirror binding sites involved in Orai1 interactions.

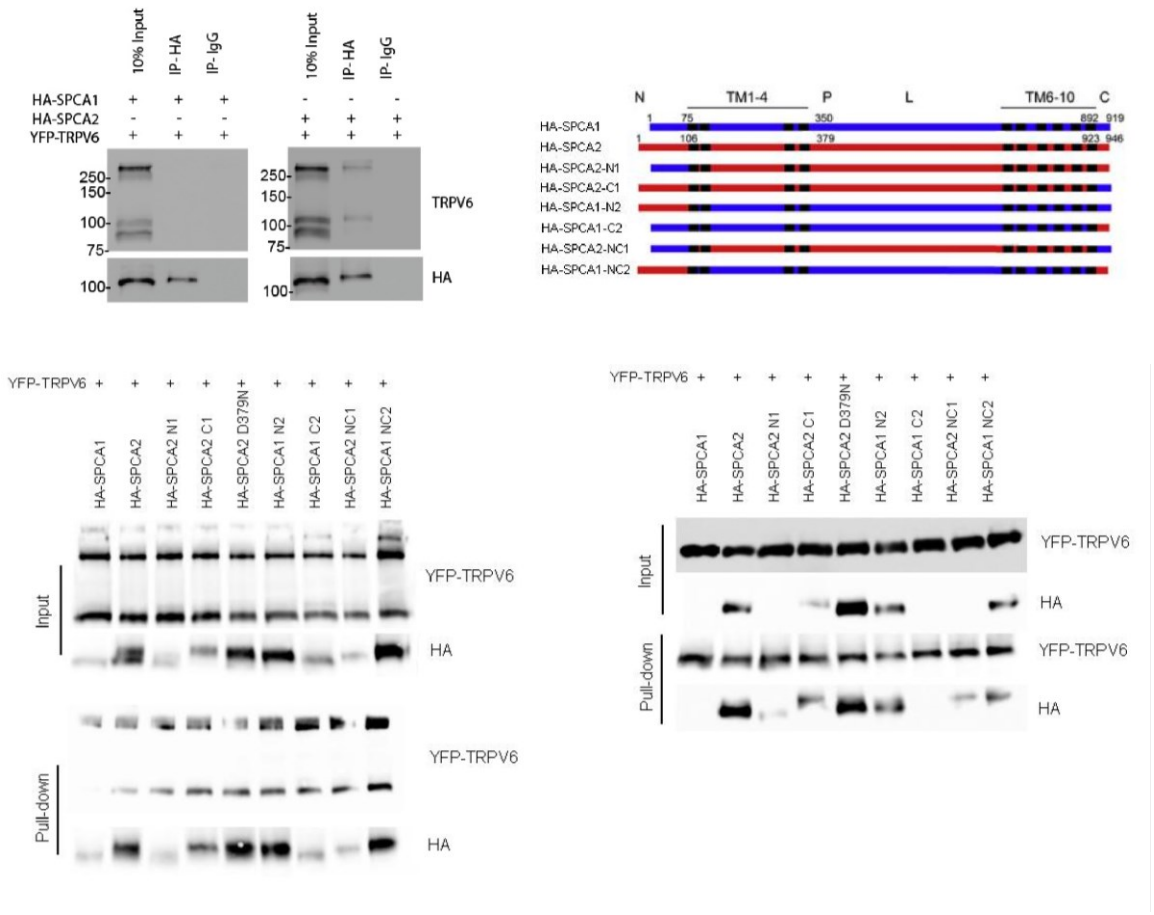

Figure 19: Coimmunoprecipitation of HA-SPCA1 or HA-SPCA2 with YFP-TRPV6 pulled down with antibody against HA (upper left panel). A detailed diagram of the expression constructs used in the lower panels is included. In order to determine the regions conferring binding specificity to SPCA2 we performed coimmunoprecipitation with antibody against either HA or GFP (bottom left and right panels, respectively.

Finally, we wanted to address the possibility that SPCA2 binding to TRPV6 has a regulatory role on channel's activity. In HEK293 cells, the strain used mattered in the effect of SPCA2-induced nuclear translocation of NFAT. We chose to work with HEK293A which seemed to have a dose-response to the amount of HA-SPCA2 transfected into the cells. YFP-TRPV6 induced NFAT translocation in approximately 80% of cells. Addition of HA-SPCA2 did not induce nuclear translocation above that of TRPV6 alone. One possible explanation for this finding is that the upper limit of this assay has been reached. Indeed, conditions involving transient transfection that induced maximal nuclear translocation reached 80% of cells in Feng et al.

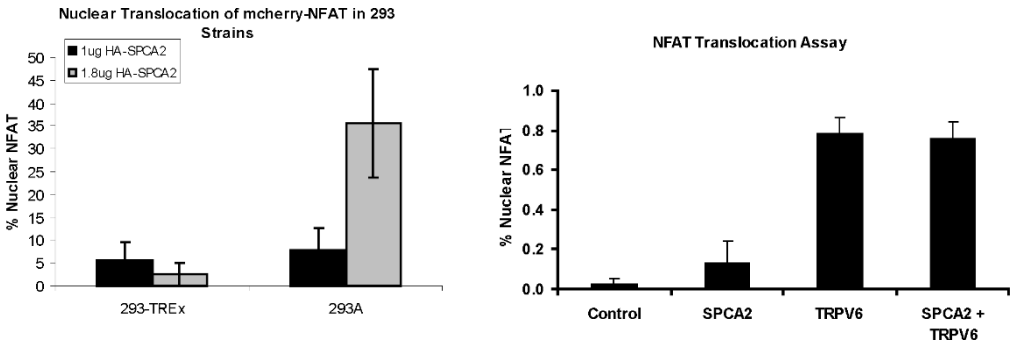

Figure 20: NFAT translocation studies in two independent HEK293 strains (left). SPCA2 failed to illicit NFAT-translocation above that of TRPV6 alone when combined with the apical calcium channel (right).

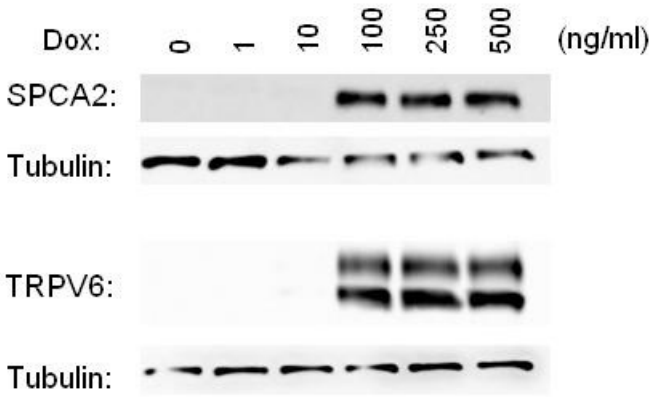

Figure 21: SPCA2 and TRPV6 are inducible in a TREx system.

In conclusion, we were unable to find evidence that SPCA2 is regulated transcriptionally by vitamin D_3 and while both SPCA1 and SPCA2 can interact with TRPV6, no upregulation of NFAT translocation was observed. Given these findings, it is difficult to support the hypothesis that SPCA2 is eliciting calcium entry in HEK293 cells by modulating TRPV6 function.

INTESTINAL MICROBIOTA

Although colorectal cancer is a disease stemming from mutations of cancer stem cells, numerous environmental factors contribute to the probability of cancer development. Indeed, microorganisms have been associated with the development of colorectal cancer and can for the first time be identified by genomics. With the emergence of high-throughput sequencing techniques, an interest has risen in the field of the microbiome, or the entirety of microorganisms living with the human body.

Over three million genes belonging to greater than 1,000 microorganisms currently comprise the human intestinal microbiota. Among prokaryotes, the three most prominent taxa (Firmicutes, Actinobacteria and Bacteroidetes) account for over 80% of the sequences attained (reviewed in de Vos and de Vos, 2012). Bacteria contributing to colorectal mutagenesis are the unusual but eminent. Enterotoxigenic *Bacteroides fragilis* (ETBF) is a gram negative causing diarrhea and colitis in the host. The secreted toxin, *B. fragilis* toxin (BTF), cleaves E-cadherin in colon enterocytes. E-cadherin suppresses the activity of the oncogene, B-catenin, which is constitutively active in nearly all colon cancers. Thus, loss of E-cadherin results in hyperproliferation of existing colon cancers. (Housseau and Sears, 2010). Similarly, *Fusobacterium nucleatum* adhesin, FadH, binds and inactivates E-cadherin thus promoting B-catenin activation (reviewed in Gagliani et al. 2014).

The microbiota is a system in delicate balance, modulated by factors including diet, host health, and immune responses. A proinflammatory environment not only alters the microbial milieu but it results in elevated ROS thus damaging enterocytes. Consequently, overgrowth of a species triggering immune responses can result in colorectal cancer as well (Gagliani et al. 2014).

Deep sequencing has picked up only a few genes belonging to fungi of the intestinal microbiome. Below, we examined the opportunistic pathogen, *Candida albicans*, which resides in the intestine of healthy individuals. Many factors are involved in the regulation of the *C. albicans* population size including probiotic *Lactobacillus plantarum* LPK (Payne et al. 2003). Although *C. albicans* has not been implicated in colon cancer development, it has been recognized that oral growths are associated with oral squamous cell carcinoma (Bakri et al. 2010). *Candida* do retain the propensity to establish a systemic infection in immunocompromised individuals. Below, we examine the relationship between *C. albicans* virulence and organellar acidification by mutagenizing two isoforms of the V-ATPase hemichannel.

CANDIDA ALBICANS AS AN OPPORTUNISTIC PATHOGEN

An opportunistic pathogen is an organism that has the ability to cause disease when conditions are favorable. *Candida albicans* resides as a commensal in our mouths, digestive tracts, and genitalia as a commensal organism. Only certain environmental cues allow *C. albicans* to establish an infection or disseminate to other sites (Calderone and Fonzi, 2001).

Crucial to the progression from commensal to pathogen is dimorphic switching. Factors that may initiate a dimorphic transition includes serum or GlcNAc, proline, increase in temperature to 37°C. Dimorphic switching is frequently associated with virulence. In a study by Susan Noble's group, 674 genes were mutagenized in *Candida albicans* and examined for bud-hyphae transition defects. Of 115 virulence-attenuated strains roughly half underwent normal dimorphic switching in the lab.

Certain virulence factors are involved in *C. albicans* dimorphism. Key in the process of germination are adhesins, a collection of proteins that allow yeast to bind host mucosa through interacting with a variety of partners including fibronectin, laminin, collagen I and IV. Certain transcription factors must also respond to changing environments and cue morphogenesis. Efg1p, Tup1p, and Rim101p are *C. albicans* transcription factors whose mutation results in pseudohyphae, constitutive hyphae or reduced hyphae, respectively. Secreted aspartyl proteases and phospholipases contribute to virulence by causing tissue damage (Calderone and Fonzi 2001).

In the gut, barriers such as tight junctions, the mucosa and secreted small antibacterial peptides are the first line of defense against the intestinal microbiota. Next, macrophages and neutrophils comprise the innate immune response and can clear microbes

by phagocytosis. Innate immune cells have the added responsibility to release pathogen antigens in order to mount an adaptive immune response.

In a murine model it was found that neutropenia was a key predisposing factor in septic candidiasis emerging from the digestive tract (Koh et al. 2008). Chemical damage to the intestinal epithelium increased the efficiency of delivery of *C. albicans* to the bloodstream yet neutropenia was essential for infection establishment. This closely mimicks epidemiological data in which primarily immunocompromised individuals are affected by this pathogen. Thus, numerous factors play a role in the overall infectivity of *Candida albicans* on both the host and pathogens side.

ESSENTIAL ROLE FOR VACUOLAR ACIDIFICATION IN CANDIDA ALBICANS VIRULENCE

The entirety of this chapter has appeared in the Journal of Biological Chemistry as a manuscript accepted for publication in 2013:

Patenaude C., Zhang Y., Cormack B., Kohler J., Rao R. (2013) Essential Role for Vacuolar Acidification in *Candida albicans*. *J Biol Chem.* **288(36)** 26256-64.

Abstract

Fungal infections are on the rise, with mortality above 30% in patients with septic *Candida* infections. Mutants lacking V-ATPase activity are avirulent and fail to acidify endomembrane compartments, exhibiting pleiotropic defects in secretory, endosomal, and vacuolar pathways. However, the individual contribution of organellar acidification to virulence and its associated traits is not known. To dissect their separate roles in *Candida albicans* pathogenicity we generated knock-out strains for the V_0 subunit *a* genes *VPH1* and *STV1*, which target the vacuole and secretory pathway, respectively. While the two subunits were redundant in many *vma* phenotypes, such as alkaline pH sensitivity, calcium homeostasis, respiratory defects, and cell wall integrity, we observed a unique contribution of *VPH1*. Specifically, *vph1*Δ was defective in acidification of the vacuole and its dependent functions, such as metal ion sequestration as evidenced by hypersensitivity to Zn^{2+} toxicity, whereas *stv1*Δ resembled wild type. In growth conditions that elicit morphogenic switching, *vph1*Δ was defective in forming hyphae whereas *stv1*Δ was normal or only modestly impaired. Host cell interactions were evaluated *in vitro* using the Caco-2 model of intestinal epithelial cells, and murine macrophages. Like wild type, *stv1*Δ was able to inflict cellular damage in Caco-2 and

macrophage cells, as assayed by LDH release, and escape by filamentation. In contrast, *vph1*Δ resembled a *vma7*Δ mutant, with significant attenuation in host cell damage. Finally, we show that *VPH1* is required for fungal virulence in a murine model of systemic infection. Our results suggest that vacuolar acidification has an essential function in the ability of *C. albicans* to form hyphae and establish infection.

Introduction

Infectious microbes have evolved a surprising array of strategies to identify and infect host cells for optimal pathogen survival and propagation. Critical to the process of microbial pathogenesis is the manipulation and response to pH. For example, *Salmonella typhimurium* evades host defense mechanisms by synchronizing the construction of the type III secretion system with macrophage lysosomal acidification (Buezon et al., 1999). The facultative intracellular fungal pathogen*Histoplasma capsulatum* survives and replicates within macrophages by inhibiting phagolysosomal fusion and regulating phagosomal pH to acquire nutrients, including iron (Hilty et al., 2008). In pathogenic yeasts, such as *Candida albicans*, pH has been implicated in proliferation, dimorphic switching between budding and hyphal forms, and virulence (Zhang and Rao, 2010). *C. albicans* is also a successful commensal, surviving in host niches with ambient pH ranging from highly acidic (pH <2) to alkaline (pH >10) (De Barnardis et al., 1998; Vylkova et al., 2011).

Central to each of these processes is the V-ATPase, a multisubunit, evolutionarily conserved proton pump that maintains pH gradients across the endomembranes of the secretory, vacuolar, and endocytic pathways in the fungal cell. The role of the V-ATPase in fungal physiology is far-reaching, impacting diverse cellular pathways ranging from

protein processing and degradation, endocytic trafficking, pH-driven exocytosis, to the transport and sequestration of metabolites, ions, and toxic drugs (Kane, 2007). Impairment of V-ATPase activity can cripple many processes important for infection: secretion of virulence factors, filamentation, and host tissue invasion, biofilm formation, countering host immunity, and tolerance to antifungal drugs (Zhang and Rao, 2010; Zhang and Rao, 2012). Not surprisingly, *C. albicans vma7* mutants, with complete loss of V-ATPase activity, are avirulent (Poltermann et al., 2005).

The pleiotropic effects of *vma* mutants lacking all V-ATPase activity, do not offer a means to dissect the individual contribution of organellar acidification to virulence and associated traits. In the budding yeast *Saccharomyces cerevisiae*, only the V-ATPase subunit *a* is expressed as two organelle-specific isoforms: Stv1p and Vph1p, that localize to the Golgi and secretory pathway, or to the vacuolar membranes, respectively. Extensive studies in this non-pathogenic model yeast have clarified the individual roles of these distinct secretory and vacuolar V-ATPase isoforms in the development of pH gradients across endomembrane compartments. The ~100 kDa *a* subunit is an integral part of the membrane embedded V_o domain where it forms two hemichannels constituting the proton conduction pathway and provides the essential positively charged counterion to facilitate dissociation of bound protons. Stv1p containing V-ATPase complexes differ from Vph1p containing enzymes in having a lower coupling efficiency of the ATP hydrolytic activity with proton transport, and lower assembly efficiency with the cytoplasmic V_1 ATPase domain (Kawasaki-Nishi et al., 2001). Consequently, in*vph1*-null mutants, Stv1p-containing V-ATPase is unable to efficiently acidify the vacuolar compartment (Manolson et al., 1992; Perzov et al., 2002). In contrast, Vph1p-containing V-ATPase complexes

appear to compensate for loss of the secretory isoform in *stv1*-null mutants, presumably in transit to the vacuolar membrane (Manolson et al., 1994).

The unique role of the Vph1p isoform offers an approach to specifically evaluate the role of vacuolar acidification in the development of virulence-associated traits in *C. albicans. S. cerevisiae vph1*-null mutants display only a partial *vma*phenotype, with no loss of function reported in a number of cellular pathways where Vph1p has a redundant role with Stv1p (Manolson et al., 1994). This functional redundancy offers the potential to mask the contribution of these pathways to virulence in *C. albicans*. With these goals in mind, we identified the two subunit *a* orthologs in *C. albicans* and confirmed their subcellular localization to the secretory and vacuolar compartments. We describe distinct phenotypes of *C. albicans stv1* and *vph1* null mutants and establish an essential role for vacuolar acidification in virulence. These novel findings extend and clarify the *in vitro* findings of Raines *et al.*, who recently demonstrated overlapping functions of Stv1p and Vph1p in *C. albicans*. Given the urgent need to expand the arsenal of antifungal drugs against the growing threat of candidiasis and other fungal infections, our findings validate the importance of the V-ATPase, and specifically, vacuolar acidification as a drug target (Zhang and Rao, 2012, Johnson et al., 2010).

EXPERIMENTAL PROCEDURES

Animal Studies

All animal work was conducted at The Johns Hopkins University according to guidelines established by the private Association for the Assessment and Accreditation of Laboratory Animal Care (AAALAC) International. The Johns Hopkins University's Animal Care and Use Committee approved all animal procedures conducted under the

protocol entitled, “Isolation of Virulence Genes in Candida” (protocol number MO10M234; approval renewed on 11/20/2012).

Yeast Strains and Plasmids

SN152 (*arg4*Δ*/arg4*Δ, *leu2*Δ*/leu2*Δ, *his1*Δ*/his1*Δ, *URA3/ura3*Δ) was generously donated by Susan Noble (UCSF) (Noble and Johnson, 2005). This background was used to create homozygous null mutants in *STV1* and *VPH1*, as well as *STV1-GFP* and *VPH1-GFP*fusion strains. An isogenic pair of wild type and homozygous *vma7*-null mutant was generously donated by Raimund Eck (Hans Knöll Institute, Germany) (Poltermann et al., 2005). pGEM-HIS plasmids containing *C. albicans STV1* and *VPH1* were kindly donated by Karlett Parra (University of New Mexico) (Raines et al., 2013).

Generation of GFP-tagged Yeast Strains

STV1-GFP and *VPH1-GFP* strains were created by transforming SN152 with their respective fusion cassettes. First, a synthetic *GFP* gene optimized for expression in *C. albicans* was inserted into pJK1027 downstream of the ClonNat cassette to generate plasmid pZR15.5. pJK1027 is an integration vector carrying nourseothricin resistance and regions homologous to the actin promoter. pJK1027 was constructed by excising a cassette containing the *CaNAT1* gene flanked by the *Ashbya gossypii TEF1* transcriptional promoter and terminator from pJK795 (Shen et al., 2005) with EcoRV and KpnI. The fragment was blunted with Klenow and ligated into pAU34 (Uhl and Johnson, 2001), which had been digested with NdeI and treated with Klenow. Next, the *GFP*-ClonNat fusion fragment was amplified from pZR15.5 with a 45 bp linker sequence attached upstream of the *GFP* sequence. Then the *STV1*open reading frame (ORF)[3] (stop codon removed) plus ∼500 bp upstream (*5′-UTR-STV1*) and ∼500 bp immediately downstream

of the ORF (*3′-UTR*) were amplified separately. Next the three PCR amplicons (*5′-UTR-STV1*, linker-*GFP*-ClonNat, and *3′-UTR*) were fused together by a one-step PCR. Finally this fusion PCR cassette was transformed to SN152 to replace one copy of the wild type *STV1*gene and generate the STV1-GFP strain YZR226. The VPH1-GFP strain was generated similarly.

Generation of Null Mutants

STV1 and *VPH1* null strains were generated as described previously (Noble et al., 2010) and confirmed by PCR amplification. Briefly, gene disruption cassettes containing either *Candida dubliniensis HIS1* or *Candida maltosa LEU2* flanked by ∼350 upstream and downstream of the *STV1* and *VPH1* genes were constructed by fusion PCR. Heterozygous deletion strains were constructed by transformation of SN152 with a *HIS1*-marked gene disruption cassette; His+ transformants were screened by colony PCR for the presence of expected 5′ and 3′ junctions of the integrated DNA. Homozygous gene disruption strains were constructed by transformation of the heterozygous knock-out strain with a *LEU2*-marked gene disruption cassette; His+ Leu+ transformants were screened for expected 5′ and 3′ junctions of the second disrupted allele, absence of the original target ORF, and the presence of *CdHIS1* and *CmLEU2* ORF. The following null strains were generated: YZR218 (*arg4*Δ*/arg4*Δ, *leu2*Δ*/leu2*Δ, *his1*Δ*/his1*Δ, *URA3/ura3*Δ,*stv1*Δ*::Leu2/stv1*Δ*::His1*) and YZR219 (*arg4*Δ*/arg4*Δ, *leu2*Δ*/leu2*Δ, *his1*Δ*/his1*Δ,*URA3/ura3*Δ, *vph1*Δ*::Leu2/vph1*Δ*::His1*).

Generation of Reintegrants

VPH1 ORF and flanking regions were cloned into pJK1027, an integration vector carrying nourseothricin resistance and regions homologous to the actin promoter. The plasmids were linearized by restriction digestion with BsrI and subsequently transformed into the appropriate knock-out strains. Transformants were selected on YPD supplemented with nourseothricin (100 μg/ml). Confirmation of reintegration was by PCR amplification and by showing a reversal of zinc hypersensitivity.

Yeast Growth

C. albicans strains were maintained on YPD plates unless specified otherwise. Sensitivity to Zn^{2+} was monitored in synthetic complete (SC) or YPD medium supplemented with $ZnCl_2$ to 0.5 mM. Sensitivity to acidic pH was conducted in SC medium buffered with 50 μM sodium citrate and adjusted to pH 2.5. Sensitivity to alkaline pH was conducted in SC medium, which was buffered with 50 mM MOPS and adjusted to pH 8. Respiration deficiency was assessed in YPEG which contained 1% Bacto-yeast extract, 2% Bacto-peptone, 3% glycerol, and 2% ethanol. Calcium homeostasis deficiency was assessed in SC medium at pH 6 supplemented with FK506 to 2 μg/ml. Sensitivity to calcofluor white was assessed on YPD supplemented with calcofluor white to 20 μg/ml.

pH Measurements

Vacuolar pH was measured with BCECF-AM (Molecular Probes, Eugene, OR), a pH-sensitive fluorophore that accumulates in the yeast vacuole (Zhang et al., 2010; Brett et al., 2005). Yeast strains were grown to mid-logarithmic phase in YPD medium. Cells were collected by centrifugation and incubated in SC containing 50 μM BCECF-AM for 25 min then washed twice before being resuspended in SC to OD 2 and transferred to a 96-well plate. Fluorescence emission at 520 nm was measured with dual excitation at 485 nm

and 450 nm in a Fluostar Optima plate reader. All measurements were taken from samples in triplicate. Vacuolar pH was calculated using a calibration curve covering pH from 4 to 8.5 as described (Brett et al., 2005).

Hyphal Development

Late exponential-phase cultures grown at 30 °C were diluted 10-fold into fresh YPD supplemented with 10% (w/v) FCS at 37 °C as described previously (Poltermann et al., 2005) to induce hyphal growth in liquid medium. Hyphal growth in solid media was induced on Spider plates as described previously (Poltermann et al., 2005).

Cell Adhesion and Damage

C. albicans were grown for 6 h from a starter culture, sonicated in a water bath to disperse clumps, and 5000 cells were applied to a monolayer of Caco-2 cells grown in a 35-mm dish for 10 days. After 30 min, culture supernatant was collected, diluted, and plated to YPD to estimate the number of non-adherent yeast cells. The Caco-2 monolayer was washed briefly five times with PBS and then cells were scraped in 1 ml PBS and the lysate was plated on YPD to calculate the number of adherent yeast cells. Data represented shows the number of adherent cells compared with the total number of viable cells used. Data shown are an average of three experiments with error bars displaying the standard error of the mean. *p* values were calculated using the Student's *t* test.

J774A.1 macrophages were grown as confluent monolayer in high glucose DMEM without sodium pyruvate supplemented with 10% FBS in 24-well plates. They were infected with the indicated *C. albicans* strains at multiplicity of infection of 5. The following morning, cellular medium was aspirated and fresh medium was applied to the monolayer. After 4 h, medium was collected, and lactate dehydrogenase activity was

measured as per manufacturer's protocol (Promega CytoTox 96 Nonradioactive Cytotoxicity Assay).

Systemic Infection

Virulence assays were performed as modified from Noble and Johnson. In short, *C. albicans* were grown overnight at 30 °C and then used to inoculate at second culture (by a 1:30 dilution). After 5 h, optical densities were determined. Cells were pelleted at 2000 rpm for 5 min and then washed once with normal saline and serially diluted to achieve 8×10^6 cells/ml for tail vein injections. 0.1 ml was injected into each of Balb/c female mice that were 8–10 weeks old. We injected 10 mice per strain and monitored death over 25 days. Mice that were moribund, showing weight loss, hunched posture, failure to groom, and/or motor deficits, were euthanized. Survival curves were analyzed using the log rank test.

RESULTS

Localization of V_o Subunit a Isoforms to Vesicular (Stv1p) and Vacuolar (Vph1p) Compartments in C. albicans

Two *C. albicans* ORFs have been annotated as V-ATPase subunit *a* *STV1* and *VPH1*(www.candidagenome.org). These two paralogs have 48.2% amino acid identity with one another. The putative CaVph1p (orf19.6863) and CaStv1p (orf19.1190) proteins share identities of 74.9 and 73.5% to their respective *Saccharomyces*orthologs. Neither ORF contains the N-terminal WKY motif that has been identified as targeting sequence for secretory pathway localization in*Saccharomyces* ortholog Stv1p (Finnigan et al., 2012), although putative CaStv1p does contain a WKY motif within a loop region. FXFXD motifs at positions 221 and 755 were previously described as the putative

localization sequences for Golgi retention of ScStv1p (Manolson et al., 1994). Putative CaStv1p also contains a FXFXD motif (822–826, FNFGD) whereas CaVph1p does not. To confirm these *in silico* predictions, we tagged each ORF with C-terminal GFP at the chromosomal locus in wild type *C. albicans*strain SN152. Consistent with bioinformatics data, live fluorescence imaging of transformed yeast showed punctate labeling for CaStv1-GFP (Fig. 1*B*), reminiscent of secretory pathway staining of Golgi, endosomes, and prevacuolar compartments in *S. cerevisiae*. CaVph1-GFP localized to the vacuolar membrane marked by the vacuolar dye FM4–64 in live cells (Fig. 1*C*), similar to *S. cerevisiae*Vph1-GFP (Manolson et al., 1994).

Redundant Roles for Stv1p and Vph1p Revealed by Lack of Some vma Phenotypes

As expected for its diverse role in pH and ion homeostasis, loss of V-ATPase function is accompanied by pleiotropic defects that include the growth sensitivity to acid or alkaline stress, calcium signaling, cell wall integrity, and cell respiration. To assess the functional redundancy of *a* subunit isoforms Stv1p and Vph1p to these processes, we generated homozygous null mutant strains *stv1*Δ*/stv1*Δ and *vph1*Δ*/vph1*Δ isogenic to *C. albicans* SN152. Vma7p is an essential subunit of the V-ATPase that drives the rotary catalytic mechanism (Nelson et al., 1994). Therefore, we used the homozygous null mutant *vma7*Δ*/vma7*Δ along with its isogenic control, to elicit the *vma* phenotype (Poltermann et al., 2005). While all strains grew well in YPD medium buffered to pH 4.0, the homozygous *vma7* mutant showed characteristic growth sensitivity at extremes of acid (pH 2.5) and alkaline (pH 8.0) media as has been reported for *S. cerevisiae vma* mutants. Mutants lacking Stv1p or Vph1p, however, showed normal or near normal growth (Fig. 2*A*). Calcium homeostasis defects in *vma* mutants are exacerbated by loss of calcineurin

signaling, resulting in synthetic lethal phenotype (Hemenway et al., 1995; Tanida et al., 1995). Addition of the calcineurin inhibitor, FK506, under conditions of mild alkaline stress (pH 6.0) resulted in nearly complete inhibition of growth in the *vma7* mutant, whereas neither *stv1* nor *vph1*mutants were affected (Fig. 2*B*). Furthermore, *vma* mutants show signs of oxidative stress and defects in cellular respiration (Manolson et al., 1994, Milgrom et al. 2007). We show that *C. albicans vma7* mutant is unable to grow on glycerol as a non-fermentable carbon source (YPEG, Fig. 2*C*). However, deletion of neither of the two V_o subunit *a*isoforms revealed any growth sensitivity on this medium (Fig. 2*C*). Similarly, slow growth of *vma7* mutant on YPD plates was further impaired by calcofluor white, an agent previously shown to cause cell wall stress, but this was not observed in*vph1*- or *stv1*-null mutants (Fig. 2*D*). We conclude that the two isoforms of subunit *a* play redundant roles in a wide range of functions attributed to the V-ATPase.

VPH1 Is Essential for Vacuolar Acidification and Function

The acidic pH established by the H^+ pumping activity of the V-ATPase is central to the function of the vacuole or lysosome in eukaryotic cells. We used the ratiometric pH indicator BCECF to measure the pH of the yeast vacuole. The acetoxymethyl form of BCECF is taken into the cell and de-esterified in the yeast vacuole, where it becomes trapped (Fig. 3*A*, *inset*) allowing quantitative estimation of pH_v in live yeast. As expected, vacuolar pH in wild type yeast was acidic, ranging from pH 5.12 ± 0.088 in SN152 and 5.54 ± 0.053 for CNC44. Loss of Vma7p resulted in significant vacuolar alkalinization by 1.43 pH units. Similarly, pH_v was increased by 1.44 pH units in the *vph1* null mutant but did not alter significantly in *stv1* mutant (pH_v 5.5). This confirms extensive studies in *S. cerevisiae* showing isoform specificity of subunit *a* in vacuolar acidification. We conclude

that, as in *S. cerevisiae*, *C. albicans* Vph1p is required for robust vacuolar acidification, and that Stv1p is not capable of compensating for loss of Vph1p.

The acidic vacuole is the major site of ion and metabolite sequestration, driven by the H^+ gradient established by V-ATPase. Thus, the *vma* phenotype includes hypersensitivity to metal ions, including Co^{2+}, Mn^{2+}, Cu^{2+}, Ni^{2+}, and Zn^{2+} (Poltermann et al., 2005). We show increased sensitivity to elevations in extracellular zinc in *vph1* and *vma7*null strains, relative to their isogenic controls (Fig. 3*B*), consistent with the absence of vacuolar acidification. Loss of Stv1p did not alter Zn^{2+} sensitivity, similar to findings in *S. cerevisiae* (Finnigan et al., 2012).

Isoform-specific Differences in the Role of V_o Subunit a in Hyphal Development

The vacuole is critical in germ tube formation and for invasive hyphal growth in *C. albicans*. Sub-apical vacuoles have been shown to rapidly fuse and enlarge, crowding out the cytoplasm, which remains confined to the advancing apical tip of the hypha (Palmer, 2011). The critical importance of cellular pH homeostasis in hyphal development was indicated by a nearly complete inability of *vma7* mutants to generate filaments in liquid Spider medium, which has mannitol as sole carbon source (Fig. 4) (Poltermann et al., 2005). However, the relative contribution of transmembrane pH gradients in the secretory and vacuolar compartments in hyphal formation is unclear. Interestingly, the *stv1* mutant showed significant reduction of nearly 40% in filamentation, with larger reduction (85%) observed in the *vph1*-null strain (Fig. 4). Because hyphal formation is reduced but not completely abolished in the absence of either subunit *a* isoform, these results suggest that Stv1p and Vph1p both contribute to germ tube formation in liquid cultures, but can compensate, at least in part, for each other.

Hyphal formation can also be visualized at the peripheral margins of yeast colonies growing on solid medium. In solid Spider medium, we observed significant differences in hyphal outgrowth between *vph1* and wild type, but not for *stv1* mutant (Fig. 5*A*, *top panel*). These differences are evident at 25× magnification of the colony periphery (Fig. 5*A*, *bottom panel*) and suggest that Vph1p is important for hyphal formation on solid media whereas Stv1p is largely dispensable. To confirm this, we also examined hyphal formation on solid YPD medium supplemented with serum. Again, the *vph1* mutant was defective in filamentation seen at the periphery of colonies, like the *vma7*-null strain (Fig. 5*B*,*top* and *bottom panels*). Taken together, our observations point to a role for Vph1p and vacuolar acidification in hyphal formation.

Host Cell Interaction Differs among V-ATPase Mutants

The intestinal mucosal barrier plays a critical role in determining virulence of *C. albicans* (Schulze and Sonnenborn, 2009). To be retained on the intestinal surface, yeast cells must adhere to epithelial membranes. Therefore, we tested whether V-ATPase mutants were defective in adhesion to a polarized monolayer of Caco-2 epithelial cells. Late log phase *C. albicans* were applied to a polarized, differentiated epithelial monolayer and allowed to attach for 30 min. Subsequently, yeasts remaining in the supernatant were collected and plated to determine if any loss in viability occurred during incubation at pH 7.4. After five washes, Caco-2 were scraped and resuspended in PBS for plating to YPD. Like *vma7*, the *stv1* mutant had a modest although statistically significant reduction in adhesion, suggesting a potential role for V-ATPase in secretion of adhesion factors (Fig. 6*A*). Adhesion of *vph1*mutants was not reduced to statistically significant levels. However, adherence does not appear to be a defining feature in the relative virulence of the strains

tested. Thus, host cell damage in *stv1* mutants was indistinguishable from wild type, as monitored by release of lactate dehydrogenase from Caco-2 monolayers exposed to yeast cells for 16 h. In comparison, loss of Vph1p did reduce cellular damage to Caco-2 cells, although this was not as drastic as seen with *vma7*mutant strain, which has a complete loss of V-ATPase activity (Fig. 6*B*).

In systemic infection by *Candida*, professional phagocytes, including macrophages, constitute the first line of host defense. Fungal cells are internalized into the phagosome, which matures into an acidic phagolysosome where hydrolytic enzymes like cathepsin B are activated. In response, environmental cues such as CO_2 concentration and pH trigger filamentation by *C. albicans*, followed by piercing of the macrophage membrane and escape. Here, we evaluate the interaction of V-ATPase mutants with cultured murine macrophage-like cells, J774A.1 (McKenzie et al., 2010). Following an overnight incubation at a multiplicity of infection of 5, wild type strains SN152 and CNC44 were able to filament robustly (Fig. 6*C*), and kill macrophage cells as evidenced by release of LDH (Fig. 6*D*). In contrast, *vma7* mutants failed to form filaments and escape macrophages, and were unable to elicit LDH release above that of control, uninfected macrophages. We observed no requirement for Stv1p in filamentation and no deficit in the ability to cause host cell damage. However, both filament formation and LDH release from macrophages were significantly attenuated in *vph1* mutants (Fig. 6, *C* and*D*).

Vph1p Is Required for Virulence in a Murine Systemic Infection Model

Previously, *vma7* mutants lacking all V-ATPase activity were shown to be avirulent in a mouse model of system infection (Poltermann et al., 2005). The distinct contributions of Vph1p and Stv1p in vacuolar acidification provided a unique opportunity to distinguish

between the relative roles of vacuolar and secretory pathway acidification by the V-ATPase in virulence. We generated a reintegrant of *VPH1* in the null strain that was verified by PCR amplification and complementation of the Zn^{2+}-sensitive phenotype (Fig. 7, *A* and *B*). Freshly grown, viable cultures (8×10^5 cells) of each of homozygous null, *VPH1* reintegrant and corresponding wild type strain SN152 strains were injected into the tail vein of 8–10 week old female Balb/c mice ($n = 10$ each) and survival was scored over 25 days (Fig. 7*C*). The reintegrant was not statistically different in virulence from wild type (p value 0.168, log rank test) (Noble and Johnson, 2005). The *stv1*-null mutant retained virulence and was also similar to wild type (p value 0.5), whereas the *vph1*-null strain failed to kill any of the mice over the course of the observed period (p value 1.7e-09).

DISCUSSION

As a master regulator of intracellular pH, the fungal V-ATPase is critical for a diverse range of cellular functions including vacuole acidification, vesicular transport, and trafficking, pH-dependent growth, metal ion homeostasis, hyphal growth, and pathogenicity. Not surprisingly, complete loss of V-ATPase activity in the *vma7* mutant of *C. albicans* leads to loss of virulence (Poltermann et al., 2005), although it is not clear which of these many functions is critical for virulence. Here, we have confirmed and extended the phenotypes of *vma7* mutants. In addition to previously known defects in alkaline pH sensitivity, endocytosis defects, and metal ion sensitivity, we also demonstrate impaired ability to deal with acid stress, calcium homeostasis, growth in non-fermentable carbon sources, and cell wall stress. Thus, the pleiotropic phenotypes of *vma* mutants observed in the model yeast *S. cerevisiae* readily extend to the pathogenic yeast *C.*

albicans. Importantly, we provide new observations showing that *C. albicans vma7* mutants fail to colonize Caco-2 intestinal epithelia and are efficiently eliminated by macrophages. Mucosal barrier damage as well as neutropenia are required for dissemination in a mouse model of GI to bloodstream transport (Dieterich et al., 2002; Koh et al., 2008).

Unlike mammalian orthologs of V-ATPase, the fungal enzyme shows little isoform diversity of the structural subunits, with the exception of the V_o subunit*a* encoded by the orthologous genes *VPH1* and *STV1* in both *S. cerevisiae* and *C. albicans*. The distinct functional properties and organellar distribution of V-ATPase complexes containing either Vph1p or Stv1p offer a unique approach to dissect the relative contributions of vacuolar and secretory pathway acidification to virulence and associated traits such as the morphogenic switch from budding cells to hyphae. Although a null mutant of Vph1p was previously examined in the fungal pathogen *Cryptococcus neoformans* and shown to be avirulent (Erickson et al., 2001), the absence of additional *a* subunit isoforms in this organism meant that the lone *VPH1* isoform was essential for all V-ATPase functions.

As a starting point for our analysis, we localized two *C. albicans* open reading frames to the vacuole and secretory pathway and evaluated their null phenotypes. We show that the vacuole-specific subunit *a* isoform, Vph1p, is required for vacuolar acidification and that this function cannot be adequately performed by the Stv1p isoform, consistent with similar observations in the non-pathogenic yeast *S. cerevisiae*. While this study was underway, Raines *et al.* also generated *stv1* and *vph1* null mutants to show that vacuolar alkalinization in *C. albicans* required Vph1p. Indeed, ATP hydrolysis and proton pumping rates were severely reduced in isolated vacuolar membranes from *vph1* mutant, but were

normal in the *stv1* mutant (Raines et al., 2013). Consistent with these observations, functions tightly linked to vacuolar acidification are disrupted in *vph1* mutants. This includes tolerance to metal ion toxicity (this work) and delivery or retention of the membrane-bound dye FM4–64 to the vacuole (Raines et al., 2013). However, many other cellular phenotypes are largely unaffected in the *vph1*- and *stv1*-null mutants, due to the functional redundancy of the two isoforms. Thus, we demonstrate characteristic *vma* phenotypes that are readily observed in the *vma7*-null strain (loss of pH tolerance, calcium homeostasis, cell wall stress, and respiratory defects) but not by either *vph1* or *stv1* mutants.

A significant and novel finding of our study is the isoform-specific requirement for Vph1p in virulence-associated traits of hyphal formation, host cell infectivity and damage measured against *in vitro* models of intestinal mucosal cells and macrophages. This specific requirement for Vph1p was confirmed by lack of virulence of *vph1*-null mutants in a murine systemic model of candidiasis. In contrast, *stv1* mutants showed no loss of virulence. Thus, vacuolar acidification may be linked to virulence in fungal pathogens. Previously, we had demonstrated a link between pH_v and *C. albicans* virulence in the mode of antifungal action of azole drugs (Zhang and Rao, 2010; Zhang et al., 2010). Loss of ergosterol from vacuolar membranes, either by mutations in the biosynthetic *erg* pathway, extraction with cyclodextrin, or by treatment with fluconazole inactivated V-ATPase, inhibited vacuolar acidification and cell growth. We showed that V-ATPase activity, vacuolar acidification, and cell growth were concomitantly restored upon feeding cells with ergosterol, independently consistent with the avirulence of *vph1* mutants shown in this work.

Although Raines *et al.* did not investigate virulence of *vph1* and *stv1*mutants, they found that loss of Vph1p resulted in deficits in hyphae formation in some media (M199) but not in others (Spider, YPD + 10% serum). The reason for the difference from our findings is unclear and may lie within strain variations or experimental protocols since a *vma* mutant was not included for comparison. Inducing media stimulate multiple signaling pathways leading to morphogenic switching, and liquid medium is a stronger inducer in many *C. albicans* mutant strains when compared with solid medium (Ernst, 2000). It would be interesting to know if the *vph1* mutant reported by Raines *et al.* retained virulence in an animal model. Further clarification could be derived from the hyphal phenotype of a *vma* mutant in the same background as their *vph1* mutant. The role of Stv1p remains elusive given the absence of specific and strong *vma* phenotypes in both model and pathogenic yeasts. The unique role of Stv1p may be unmasked under specific conditions such as glucose starvation, known to cause preferential dissociation of Vph1p containing V-ATPase complexes (Kawasaki-Nishi et al., 2001). Indeed, we did observe a significant decrease in hyphal formation in the *stv1* mutant grown in liquid Spider medium. Recently, Kane and coworkers used a Golgi-localized pH reporter to show that luminal pH becomes more acidic rather than alkaline upon loss of *S. cerevisiae* Stv1p (Tarsio et al., 2011). This unexpected acidification was even more pronounced in *vma* mutants with complete loss of V-ATPase activity, suggesting compensatory changes in organellar pH homeostasis that remain poorly understood.

Why is pH_v important for fungal pathogenesis? We know that pH homeostasis is crucial for the ability to sense and adapt to pH changes in various host niches, generate or transduce morphogenetic signals for yeast to hyphal differentiation, and to maintain vital

secretory and endocytic pathways necessary for the secretion of virulence factors. V-ATPase may be responsible for assisting in metabolic signaling events that trigger hyphal inducing genes, as suggested by Poltermann *et al.* who attributed differences in hyphal phenotype induced by Spider and serum media to unique contributions from MAPK or cAMP signaling pathways. It is known that the Rim/Pal proteins that are required for ambient pH signaling and alkaline pH response interact with ESCRT/Vacuolar Protein Sorting components Vps28 and Vps32 (Cornet et al., 2009). Deletion of *VPS28* and *VPS32* alters pH_v (Brett et al., 2011), confers sensitivity to alkaline pH growth, and reduces virulence of *C. albicans* (Cornet et al., 2005), suggestive of a role for pH_v in the Rim/Pal signaling pathway. Alternatively, V-ATPase may be necessary for tip growth to establish polarity and germ tube formation. This is supported by *Neurospora crassa vma-1* mutants that exhibit a hyperfilamentation phenotype where the hyphae have increased branching and decreased persistence at polarity growth sites (Bowman et al., 2000). Furthermore, there is consistent evidence that antifungal drugs that disrupt pH_v also block hyphal formation. Thus, fluconazole blocks yeast-to-hyphal transition (Ha and White. 1999), and inhibits V-ATPase by depleting membranes of ergosterol, leading to alkalization of the vacuole (Zhang and Rao, 2010). Similarly, amiodarone exerts its antifungal effects by alkalinizing the vacuole, and at the same concentrations, also inhibits hyphal formation in *C. albicans* (Gamarra et al., 2010). The molecular mechanism underlying this phenotype was linked to transcriptional changes in genes regulating hyphal growth. Specifically, *UME1*, an inducer of hyphal development, showed no expression in the presence of amiodarone whereas the transcription factors *TUP1*, *NRG1*, and *RFG1*, that act as negative regulators of the morphogenetic switch, were all up-regulated in

amiodarone (Gamarra et al., 2010). Future work may identify specific contributions of pH_v and distinguish between potential roles in pH sensing and response.

Acknowledgment

We thank Suzanne Noble (UCSF) for generously providing strains and help with mutant strain construction.

R01AI065983R01 GM52414R21 AI064715National Institutes of Health

Footnotes

↵* This work was supported, in whole or in part, by National Institutes of Health Grants R01AI065983 and R01 GM52414 (to R. R.), R21 AI064715 (to J. K.), and Training Grant 5T32DK007632 (to C. P.).

```
T-COFFEE, Version_9.03.r1318 (2012-07-12 19:05:45 - Revision 1318 - Build 366)
Cedric Notredame
SCORE=93
*
 BAD  AVG  GOOD
*
Vph1p     :  93
Stv1p     :  93
cons      :  93

Vph1p       1 M--------------PEKEEAVFRSADMSLVQLYVPTEVARDIIY   31
Stv1p       1 MSPIRLSENSVLSSNNESNEAIFRSAPMTLVQFYVTIELARDMVG   45
cons        1 *              *.:**:**** *:***:**. *:***::    45

Vph1p      32 KVGQLDIIQFRDLNSKINEFQRSFVKELRKLDNVERQFNLFKREL   76
Stv1p      46 VLGKLGNVQFRDLNSKLTPFQRTFITELRSIDGLVSQLDFLH-SI   89
cons       46 :*:*. :********:. ***:*:.***.:*.:  *:::::: .:   90

Vph1p      77 DV------RDIPIKLFPYDLDNVPPQTEIDELIEGSDLLEERVIQ  115
Stv1p      90 MIKQNTIKSDLYVNL-HADMKPLPTSSEIDNIKTRLSEFYERIKH  133
cons       91 :       *: ::*   *:. :*..:***::    . : **: :  135

Vph1p     116 LRDSVETLYEKEKYLKQFKYTIQAVNNFFAVQ----------GET  150
Stv1p     134 LDQSYNNLDRKRLKFIENRCVLNSLNEFHRSNLVGGGYDDEHTED  178
cons      136 * :* :.* .*.  : : : .::::*:*.  :           *   180

Vph1p     151 TNDNEETALLSQLESGGATSGGGGDARSGSSF--ISGVINRDKVG  193
Stv1p     179 ADYDDNAALLNEQRNHSLEIGYEAHNLDDISFNSLAGTIARDKVP  223
cons      181 :: ::::***.: .. .  *  ..  .. **  ::*.* ****   225

Vph1p     194 VLQQILWRVLRGNLYYHNEDLPEEIYDFKNN-TYVAKSSFIIFSH  237
Stv1p     224 ILRNILWRVLRGNLYFHDIALDDEFPATESSMDLVHKNVFIIFIH  268
cons      226 :*::***********:*:  * :*:  :.. : * *. **** *  270

Vph1p     238 GSLIRERIRKICESLDAELY-NVDSTSALRREQLDDVNTKTTDLS  281
Stv1p     269 GDFLRTRVRKIIQSLDGILFDNATGGSVARNETLTEINGKIEDLN  313
cons      271 *.::* *:*** :***. *: *. . *. *.* * ::* *  **.  315

Vph1p     282 TVLGESENALNSELIAISRDLAKWWEIIAREKAVYKAMNNCDYDN  326
Stv1p     314 NVVQTTKDQLVTELMIFQELYPDYCYIVQREKLIYETLNKFDEDS  358
cons      316 .*:  ::: * :**: :..  ..:  *: *** :*:::*: * *.  360

Vph1p     327 SRKTLIAEGWTPTDSITELTTA----------------------  348
Stv1p     359 TRRCLVGEGWIPTNDFDKIRLALRNLIRQKTRRDGSDRDSNESVN  403
cons      361 :*: *:.*** **:.: ::  *                       405

Vph1p     349 -------------------------IQEYDASQSVPTIINVLDTN  368
Stv1p     404 ISESIATETSLFAIDDSDHELTGFEIEDEDEVGSLIAVVNELATN  448
cons      406                          *:: *   *: :::* * **  450

Vph1p     369 KTPPTYTRTNKFTYAFQAICDAYGVPKYKEINPGLPTIVTFPFMF  413
Stv1p     449 RTPPTFHKTNKFTAAFQSIIDAYGIATYQEVNPGLATIITFPFMF  493
cons      451 :****: :***** ***:* ****:..*:*:****.**:******  495

Vph1p     414 AIMFGDLGHGFIVTLAAAALVLNEKKLNAMK-KDEIFDMAYTGRY  457
Stv1p     494 SIMFGDLGHGFIVFLMAIYLILNEVRFGAMRNRDEIFDMAFTGRY  538
cons      496 :************ * *  *:*** ::.**: :******:****  540

Vph1p     458 VLLLMGVFSMYTGFIYNDVFSRSMSIFKSGWEW--PEKFNV--GE  498
Stv1p     539 IILLMGVFSMYTGLIYNDIFSKSMAIFSSGWKYVIPENYDATKGA  583
cons      541 ::***********:****:**:**:**.***::  **:::.  *  585

Vph1p     499 TIYAKYVG--TYSIGLDPAWHGTENALLFSNSYKMKLSILMGYIH  541
Stv1p     584 TLVAEKIAGKVYPFGLDWAWHGTENNLLFTNSYKMKLSVLMGYTH  628
cons      586 *: *: :.  .*.:*** ******* ***:********:**** *  630

Vph1p     542 MSYSYVFSLVNYTYFNSMIDVIGNFIPGLLFMQGIFGYLSLCIVY  586
Stv1p     629 MNYSLMFSLVNYLFFKSRVDIIGNFIPGFLFMQSIFGYLALTIVY  673
cons      631 *.** :****** :*:* :*:*******:****.*****:* ***  675
```

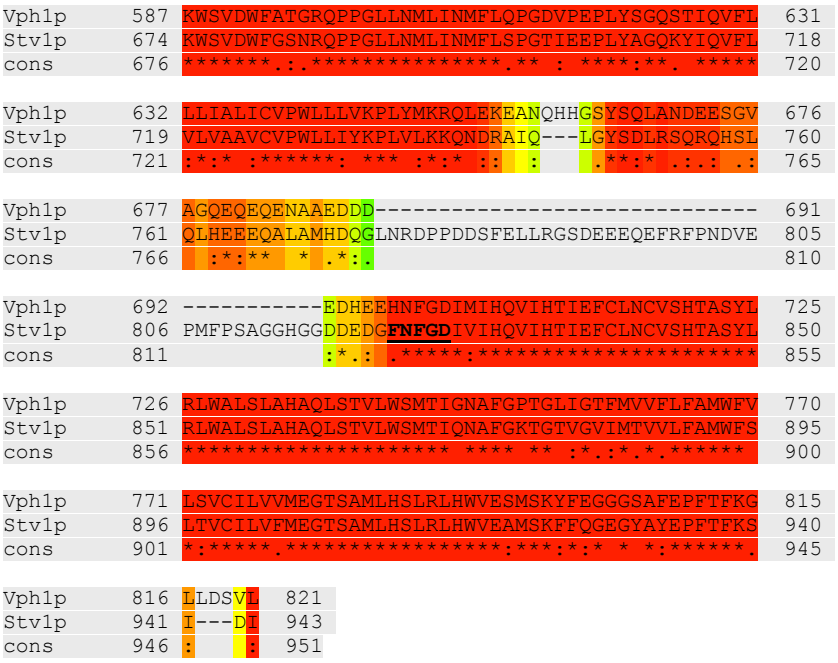

Figure 22: Multiple sequence alignment of STV1 and VPH1 genes (Candida albicans).

Vph1p *Candida albicans*

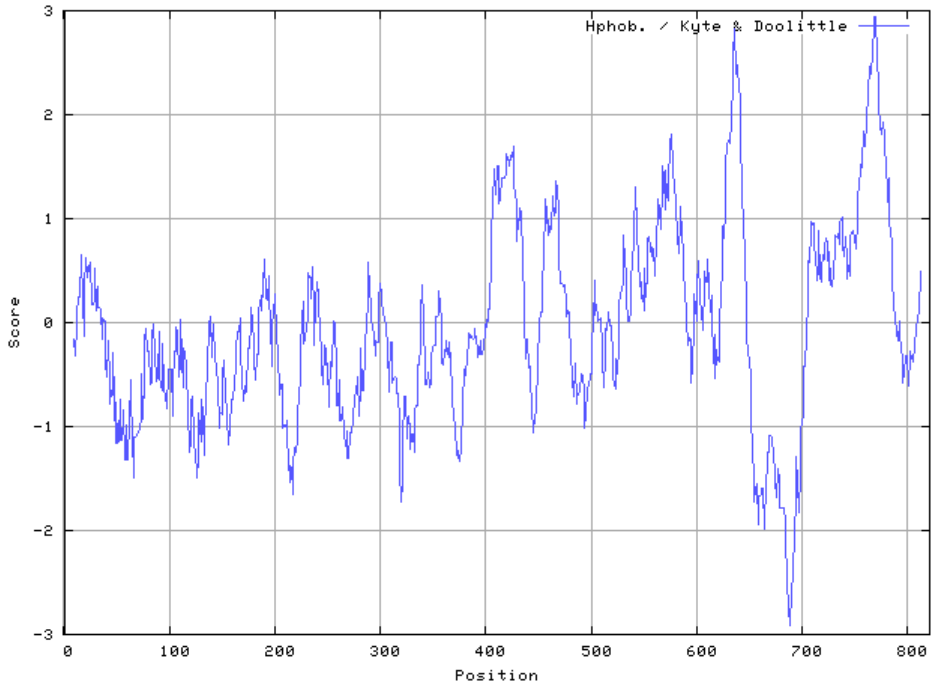

Stv1p *Candida albicans*

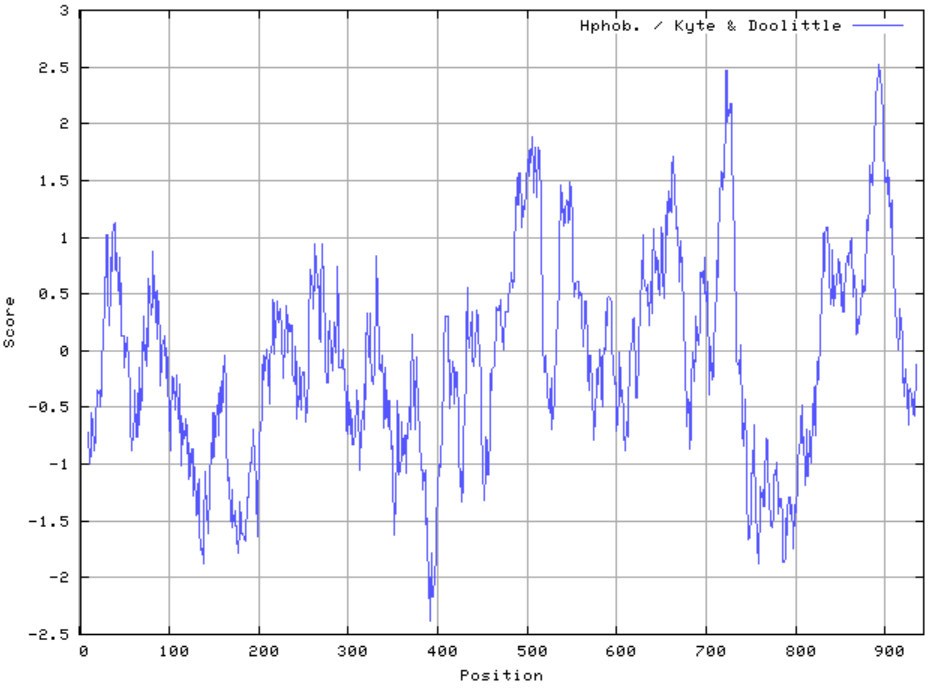

Figure 23: Hydrophobicity plots calculated with a window size of 19 using the ProtScale (Gasteiger et al. 2005) on ExPASy.org

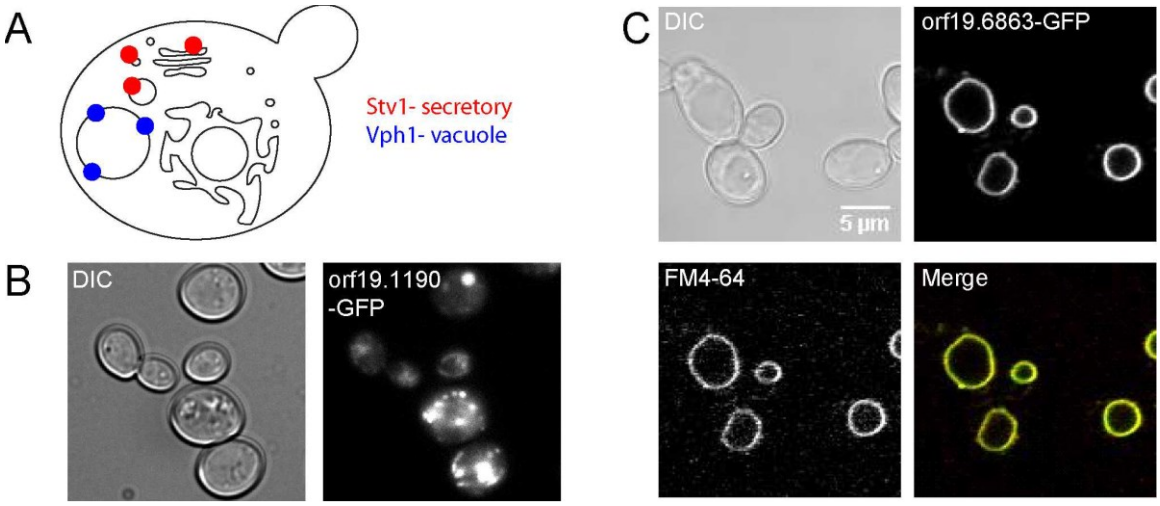

Figure 24: CaStv1p and CaVph1p localize to the secretory pathway and the vacuole, respectively. A. Diagram of budding yeast showing expected localization of VO a isoforms to the vacuole (Vph1p) and the Golgi and post-Golgi compartments (Stv1p), based on distribution of S. cerevisiae orthologs. Each C. albicans candidate ORF was cloned and C-terminal GFP-fusion constructs were expressed in WT cells. B. C. albicans ORF19.1190-GFP showed a punctate distribution consistent with secretory pathway morphology in yeasts. C. GFP-tagged ORF19.6863 localized to the vacuole as marked by the vacuolar dye FM4-64 (Data obtained by Y.Zhang).

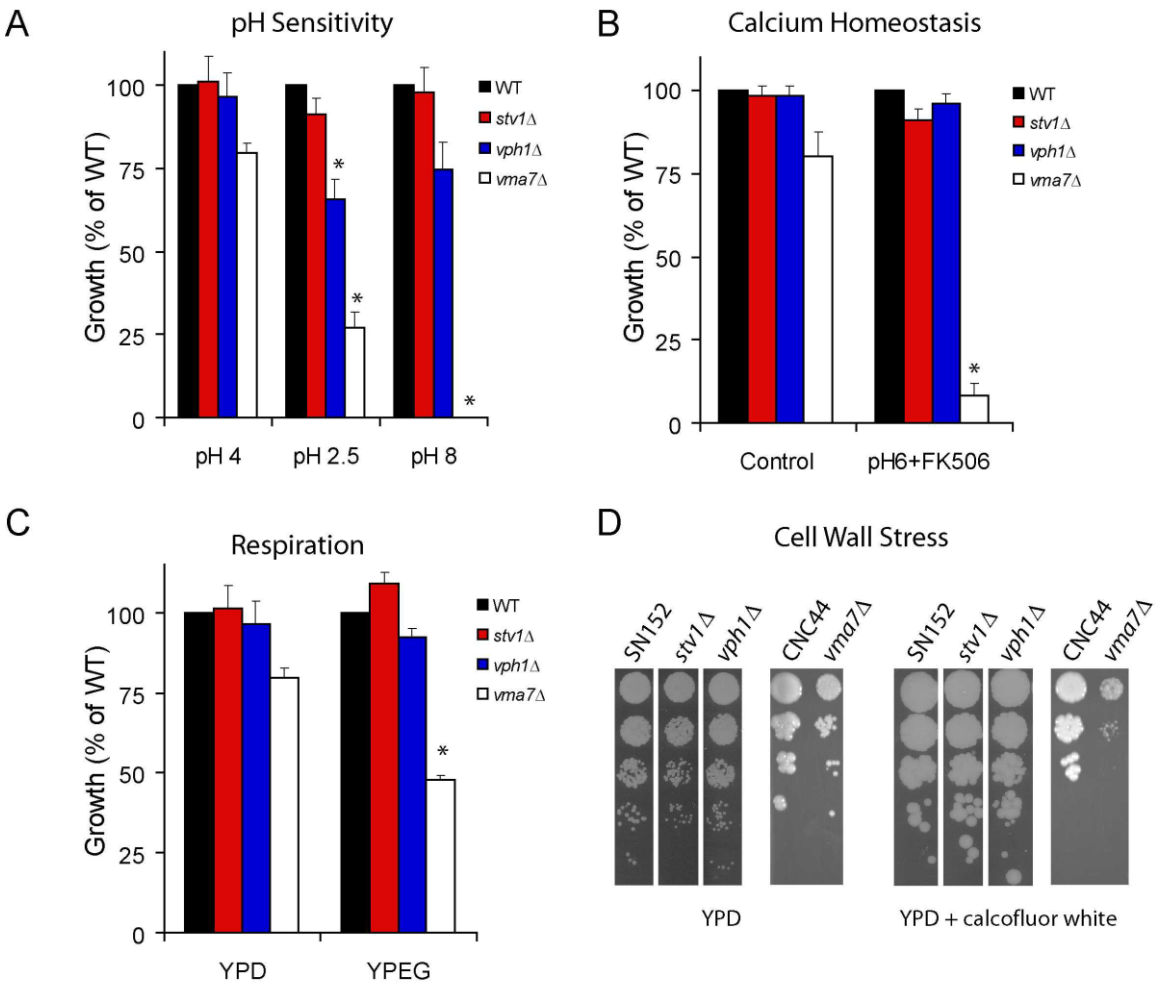

Figure 25: Redundant roles of CaStv1p and CaVph1p. Phenotypes of C. albicans homozygous null mutants vph1Δ and stv1Δ were evaluated along with vma7Δ and their respective isogenic wild type strains. Cultures were incubated at 30°C for 24 h and growth (Abs600) was expressed as percentage of the isogenic wild type control. A. Growth in response to acid (pH 2.5) and alkaline (pH 8) stress was similar to wild type in stv1Δ mutants, and mildly affected in vph1Δ, compared to the vma7Δ strain, which showed little or no growth under extremes of pH. B. Ca^{2+} stress was elicited in medium buffered to pH 6 and supplemented with the calcineurin inhibitor FK506 (2 µg/ml). No growth sensitivity was observed in stv1Δ and vph1Δ strains, whereas vma7Δ showed pronounced inhibition of growth. C. Respiratory defect was monitored in YPEG medium containing non-fermentable carbon sources. Relative to the vma7Δ, which showed significant respiration defects, stv1Δ and vph1Δ strains showed no loss of growth on non-fermentable carbon sources. D. Response to cell wall stress was monitored on YPD plates supplemented with calcofluor white (20 µg/ml). No growth sensitivity to calcofluor white was observed in stv1Δ and vph1Δ strains, in contrast to the vma7Δ strain (Panel a-c obtained by Y.Zhang).

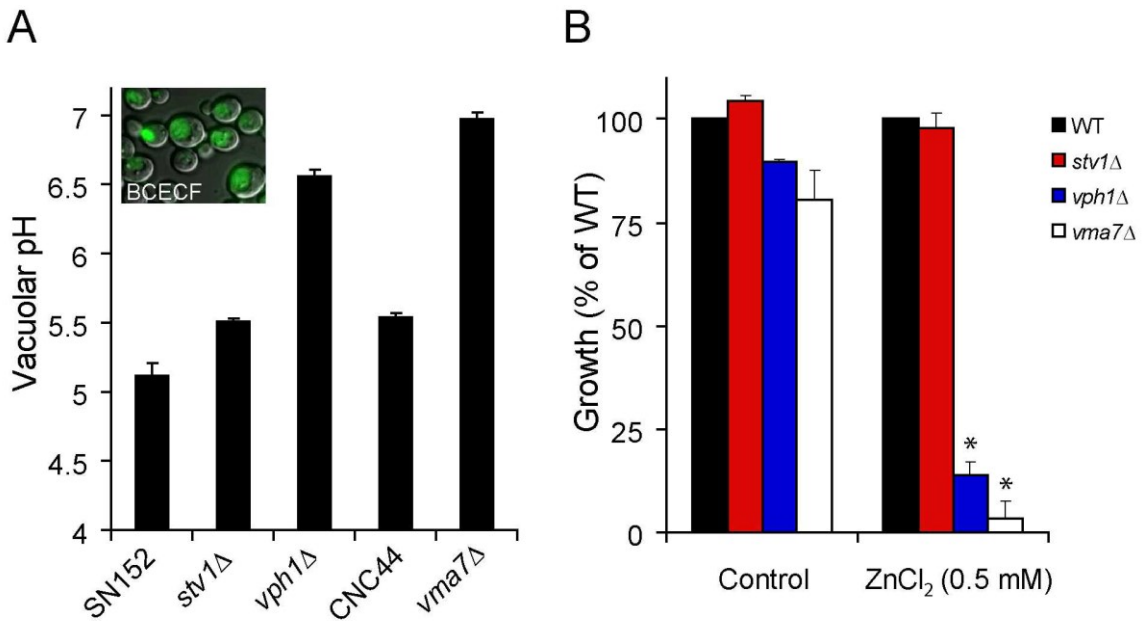

Figure 26: ***Isoform-specific role for CaVph1p in vacuolar acidification and zinc tolerance. A.*** *Vacuolar pH was measured using the ratiometric fluorescent dye BCECF-AM, which is de-esterified and accumulates inside the vacuoles of live yeast (inset) and pH_v was calculated as described in Methods. Loss of Stv1p did not significantly alter acidification of the vacuole. In contrast, loss of Vph1 resulted in large (1.4 pH unit) vacuolar alkalization, similar to that seen in the vma7Δ mutant.* ***B****. Vacuolar sequestration of toxic cations was assessed by evaluating Zn^{2+} toxicity in SC medium. Growth of homozygous null mutant strains is presented as a percentage of the isogenic wild type strain. Both vma7Δ and vph1Δ strains were hypersensitive to elevated zinc concentrations (0.5 mM) whereas stv1Δ was similar to WT (data obtained by Y.Zhang).*

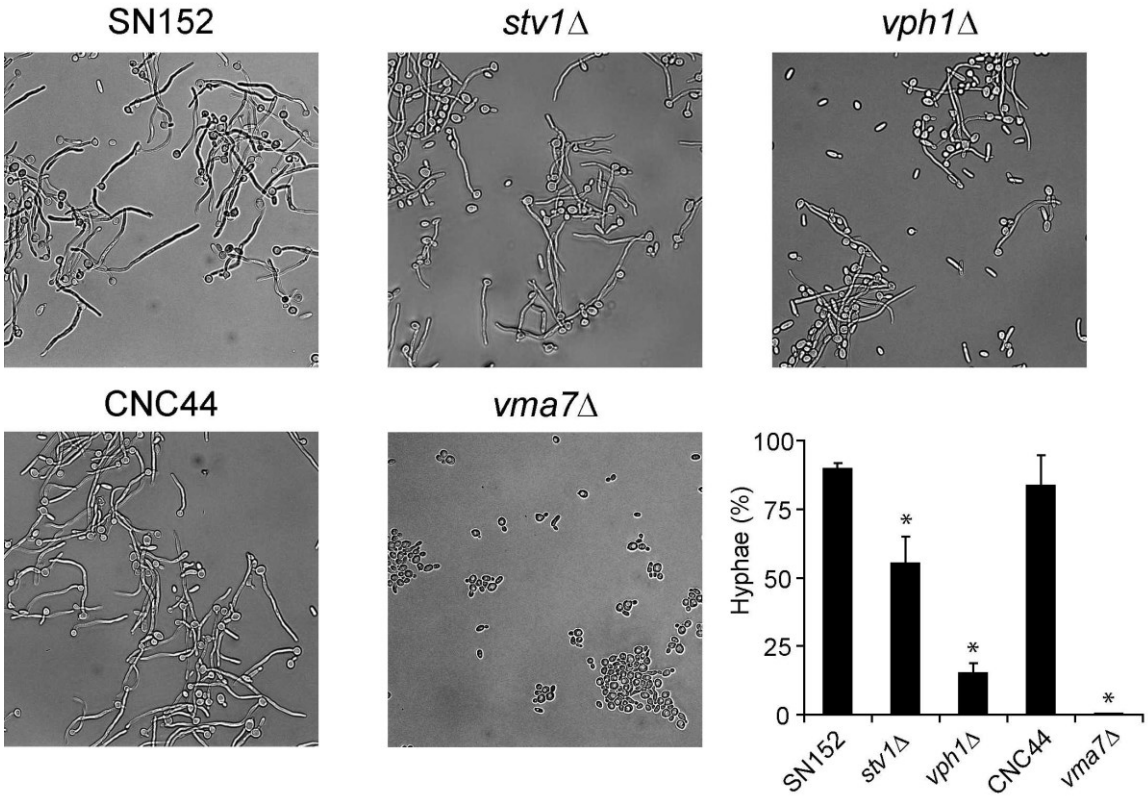

Figure 27: ***Impairment of morphogenic switching in V-ATPase mutants.*** *C. albicans was cultured in liquid spider medium for four hours and the number of cells showing hyphal development was determined by microscopic examination. In the wild type strain SN152, the majority of buds showed emergent hyphae (89%). Hyphal formation was decreased in stv1Δ to 55% and in vph1Δ to 15% of yeast cells. Nearly complete absence of morphogenic switching was observed in vma7Δ (0.3% compared to 83% in control strain CNC44) (Data obtained by Y.Zhang).*

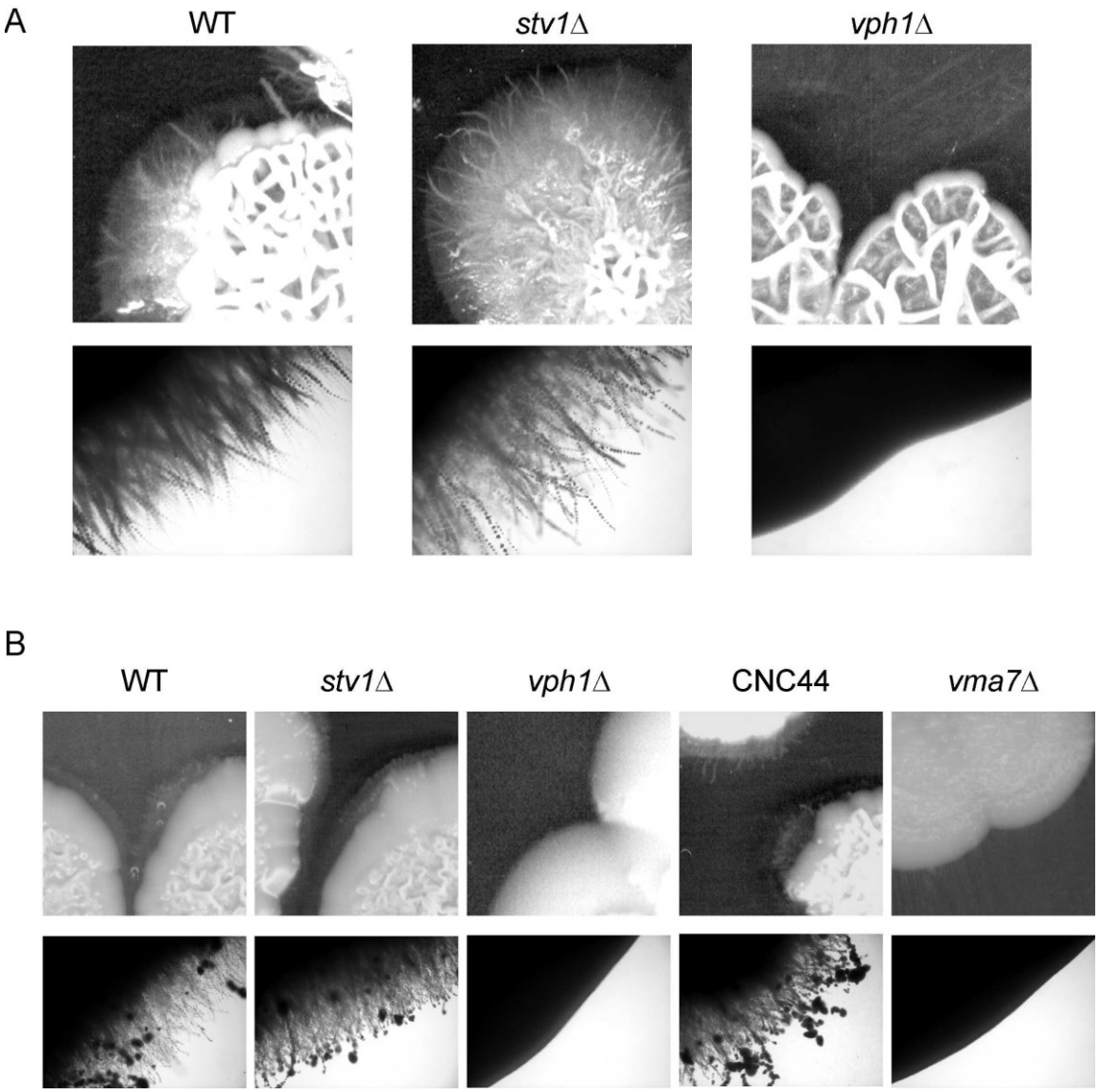

Figure 28: ***Hyphal growth on solid medium is impaired in vph1Δ mutants.*** *Colony morphology of V-ATPase mutants was monitored on* ***A.*** *solid Spider, and* ***B.*** *solid YPD plates supplemented with FBS. In both conditions, peripheral hyphae were not observed in colonies of the vph1Δ strain, similar to vma7Δ, after a period of 14 days (data obtained by Y.Zhang).*

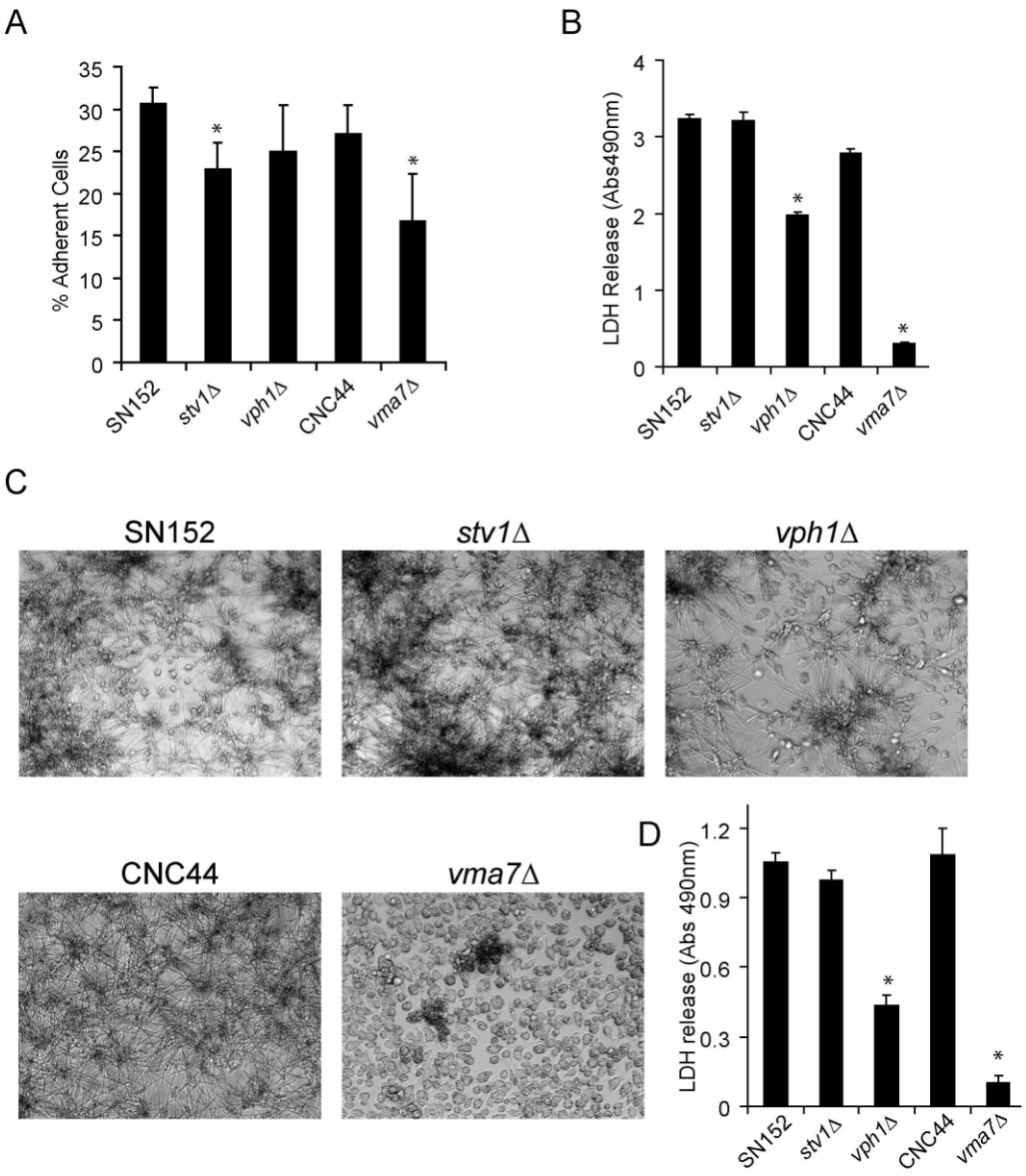

Figure 29: ***V-ATPase mutants have different effects on host cell infectivity in vitro. A.*** *Infection from C. albicans is initiated by mucosal damage or invasion. V-ATPase mutant strains were tested for defects in host adhesion by applying 5000 yeast cells to Caco-2 monolayers for 30 minutes. The percentage of adherent cells was calculated relative to the total number of viable cells as described in Methods. During this time approximately 31% (SN152) or 27% (CNC44) of WT cells adhered to the intestinal epithelial cells. The percentage of adhering cells in stv1 (23%) and vma7 (17%) strains was decreased, but the reduction was not statistically significant in vph1 mutants (27%).* ***B.*** *Host cell damage was evaluated by measuring release of the cytosolic enzyme LDH after overnight incubation of Caco-2 monolayers with C. albicans. LDH release was significantly reduced in vph1 (to 60.9% of WT) and vma7 (to 11% of WT) but not stv1 mutants. Control cells were not exposed to yeast.* ***C.*** *The ability of C. albicans to escape phagocytosis by macrophages was monitored in V-ATPase mutants and their wild type controls after incubation of yeast cells with J774A.1 cells as described in Methods.* ***D****. LDH release from J774A.1 cells after overnight incubation with C. albicans yeast was reduced in vph1 (41.1% of WT) and vma7 (9.4% of WT) mutants, consistent with defects in the ability to damage and escape from macrophages (panel c and d obtained by Y.Zhang).*

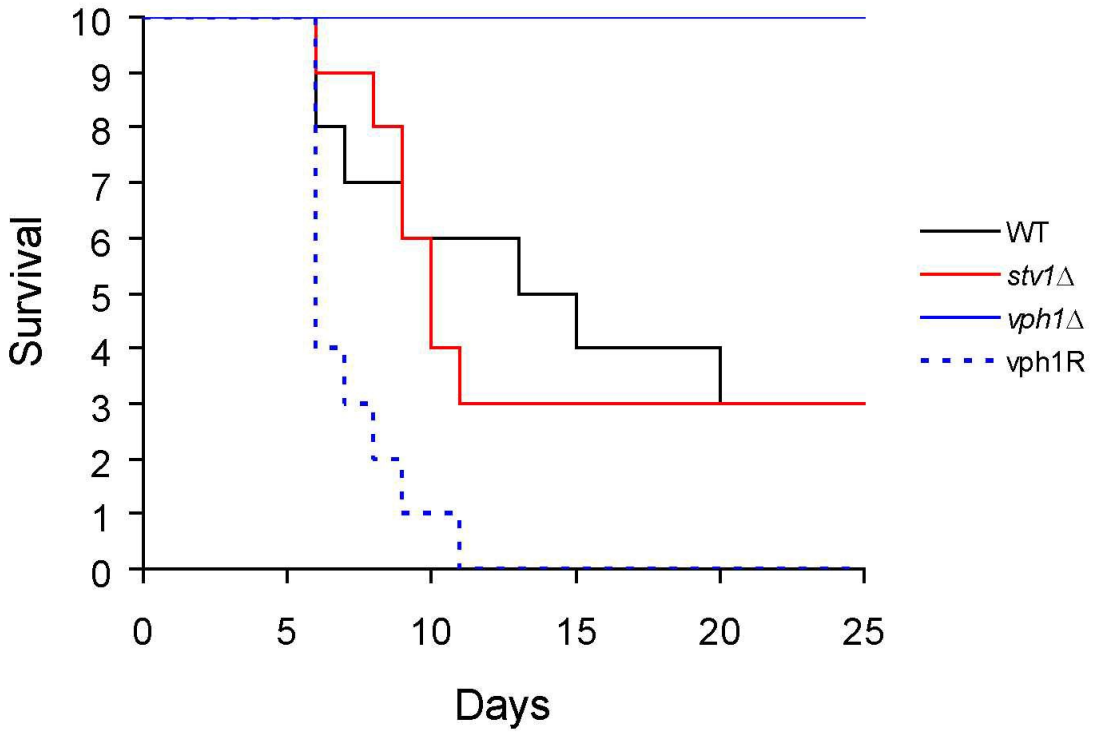

Figure 30 ***Vph1p is required for murine systemic infection****. C. albicans blastoconidia (8x10^5), from the indicated strains, were injected into the tail vein of female Balb/c mice and virulence (defined by death or moribund phenotype) was monitored over a period of 25 days. Virulence of C. albicans was not decreased in stv1Δ relative to WT. In contrast, vph1Δ was avirulent. Virulence was restored by reintegration of VPH1 gene (vph1R).*

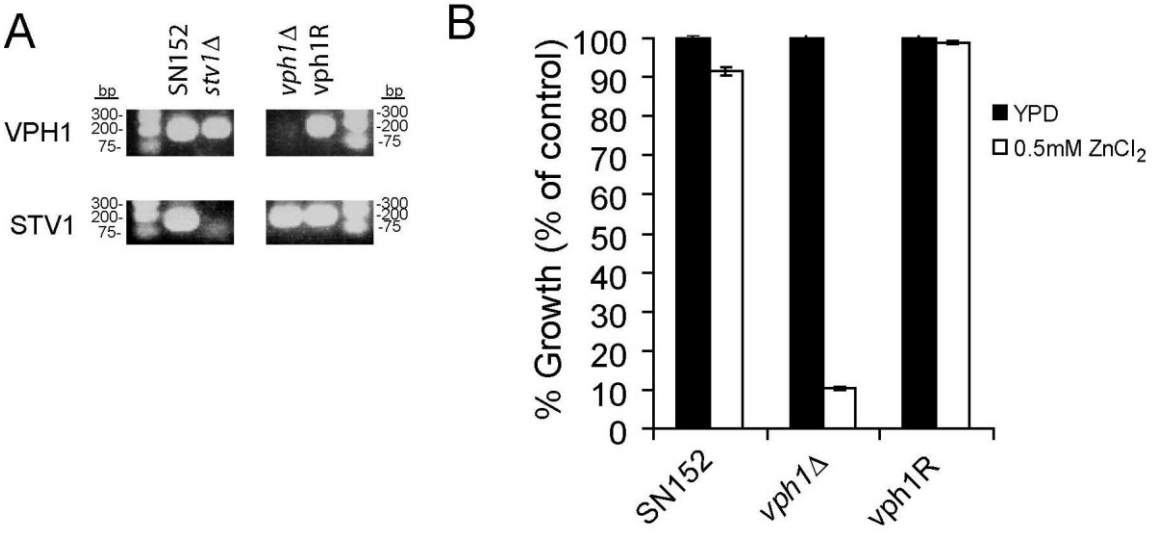

Figure 31: A) PCR analysis of genomic DNA showing deletion of VPH1 and STV1 in the null strains, and reintegration of VPH1 as indicated (B) Reversal of Zn2+ sensitivity in the VPH1 reintegrant.

BIBLIOGRAPHY

Antebi A. and Fink G.R. (1992) The yeast Ca(2+)-ATPase homologue, PMR1, is required for normal Golgi function and localizes in a novel Golgi-like distribution. *Mol Biol Cell*. **3(6)** 633-54.

Arab N. and Ghishan F. (1989) Vitamin D-Regulated, ATP-Dependent Calcium Transport by Intestinal Golgi Vesicles during Maturation in the Rat. *Pediatric Research* **26** 58-62.

Araki N., Lee T., Matsubara H., Takashima Y. (1993) An improved technique for observing both membranous organelles and cytoskeleton in saponin-extracted cells. *J Electron Microsc (Tokyo)* **42(1)** 51-4.

Barker N. (2014) Adult intestinal stem cells: critical drivers of epithelial homeostasis and regeneration. *Nature Reviews Molecular Cellular Biology* **15,** 19-33.

Benn B.S., Ajibade D., Porta A., Dhawan P., Hediger M., Peng J., Jiang Y., Oh G.T., Jeung E., Lieben L., bouillon R., Carmeliet G., and Christakos S. (2008) Active Intestinal Calcium Transport in the Absence of Transient Receptor Potential Vanilloid Type 6 and Calbindin D9k. *Endocrinology* **149(6)** 3196-205

Berridge, M.J. (1995) Calcium signaling and cell proliferation. *BioEssays* **17(6),** 491-500.

Berridge, M.J. (2012) Cell Signaling Biology: Cell Cycle and Proliferation. 9-1 - 9-42.

Beuzon CR, Banks G, Deiwick J, Hensel M, and Holden DW (1999) pH-dependent secretion of SseB, a product of the SPI-2 type III secretion system of *Salmonella typhimurium*. *Mol. Microbiol*. 33:806-816.

Bowman EJ, Kendle R, Bowman BJ. (2000) Disruption of *vma-1*, the gene encoding the catalytic subunit of the vacuolar H^+-ATPase, causes severe morphological changes in *Neurospora crassa*. *J Biol Chem*. 275: 167-76.

Brabletz T., Hubek F., Spaderna S., Schmalhofer O., Hiendlmeyer E., Jung A., Kirchner T. (2005) Invasion and Metastasis in Colorectal Cancer: Epithelial-Mesenchymal Transition, Mesenchymal-Epithelial Transition, Stem Cells and B-Catenin. *Cells Tissues Organs* **179** 56-65.

Brennan S.C., Thiem U., Roth S., Aggarwai A., Fetahu I.S., Tennakoon S., Gomes A.R., Brandi M.L., Bruggerman F., Mentavern R., Riccardi D., and Kallay E. (2013) Calcium sensing receptor signaling in physiology and cancer. *BBA- Molecular Cell Research* **7** 1732-44.

Brett C.L., Kally L., Hua Z., Green R., Chyou A., Zhang Y., Graham T.R., Donowitz M., Rao R. (2011) Genome Wide Analysis Reveals the Vacuolar pH-stat of *Saccharomyces cerevisiae. PLos ONE* **6** 217619.

Brett, C.L., Tukaye, D.N., Mukherjee, S., and Rao, R. (2005). The yeast endosomal Na+K+/H+ exchanger Nhx1 regulates cellular pH to control vesicle trafficking. *Mol Biol Cell* 16:1396-1405.

Bryant D.M. and Stow J.L. (2004) The ins and outs of E-cadherin trafficking. *Trends in Cell Biology* **14(8)** 427-34. Circu M.L. and Aw T.Y. (2010) Reactive Oxygen Species, Cellular Redox Systems and Apoptosis. *Free Radic Biol Med.* **48(6)** 749-62.

Calderone R.A. and Fonzi W.A. (2001) Virulence factors of *Candida albicans*. *Trends in Microbiology* **9(7)** 327-35.

Carmona A., Deves G., Roudeau S., Cloetens P., Bohic S. and Ortega R. (2009) Manganese Accumulates within Golgi Apparatus in Dopaminergic Cells as Revealed by Synchrotron X-ray Fluorescence Nanoimaging. *ACS Chem Neurosci* **1(3)** 194-203.

Centeno V., de Barboza G.D., Marchionatti A., Rodriguez V., and de Talamoni N.T. (2009) Molecular mechanisms triggered by low-calcium diets. *Nutrition Research Reviews* **22(2)** 163-74.

Chakrabarti G., Zhou X., and McClane B.A. (2003) Death Pathways Activated in CaCo-2 Cells by *Clostridium perfringens* Enterotoxin. *Infect. Immun*. **71(8)** 4260-70.

Cialfi S., Oliviero C., Ceccarelli S., Marchese C., Barbieri L., Biolcati G., Uccelletti D., Palleschi C., Barboni L., De Bernardo C., Grammatico P., Magrelli A., Salvatore M., Taruscio D., Frati L., Gulino A., Screpanti I., and Talora C. (2009) Complex multipathways alterations and oxidative stress are associated with Hailey-Hailey disease. *British Journal of Dermatology* **162(3)** 518-26.

Cornet M., Bidard F., Schwarz P., Da Costa G., Blanchin-Roland S., Dromer F., Gaillardin C. (2005) Deletions of endocytic components VPS28 and VPS32 affect growth

at alkaline pH and virulence through oth RIM101-dependent and RIM101-independent pathways in *Candida albicans*. *Infect. Immun.* **73** 7977-87.

Cornet M., Richard M.L., Gaillardin C. (2009) The homologue of the *Saccharomyces cerevisiae RIM9* gene is required for ambient pH signaling in *Candida albicans*. *Res Microbiol.* **160** 219-23.

Cross B.M., Hack A., Reinhardt T.A., and Rao R. (2013) SPCA2 regulates Orai1 trafficking and store independent Ca2+ entry in a model of lactation. *PLoS ONE*

Culotta V.C. and Daly M.J. (2013) Manganese Complexes: Diverse Metabolic Routes to Oxidative Stress Resistance in Prokaryotes and Yeast. *Antioxidants & Redox Signaling* **0(0)** 1-12.

De Bernardis F, Mühlschlegel FA, Cassone A, and Fonzi, WA. (1998) The pH of the Host Niche Controls Gene Expression in and Virulence of *Candida albicans. Infect. Immun*. 66: 3317-3325.

de Vos, W. M. and de Vos, E. A. (2012), Role of the intestinal microbiome in health and disease: from correlation to causation. Nutrition Reviews, 70: S45–S56

Dieterich C, Schandar M, Noll M, Johannes F-J, Brunner H, Graeve T, Rupp S. (2002) *In vitro* reconstructed human epithelia reveal contributions of *Candida albicans EFG1* and *CPH1* to adhesion and invasion. *Microbiology* 148: 497-506.

Dode, L., Anderson J.P., Vanoevelen J., Raeymaekers L., Missiaen L., Vilsen B., and Wuytack F. (2006) Dissection of the Functional Differences between Human Secretory

Pathway Ca2+/Mn2+-ATPase (SPCA) 1 and 2 Isoenzymes by Steady-state and Transient Kinetic Analyses. *J. Biol. Chem.* **281** 3182-9.

Dolman N.J., Gerasimenko J.V., Gerasimenko O.V., Voronina S.G., Peterson O.H., and Tepikin A.V. (2005) Stable Golgi-mitochondria complexes and formation of Golgi calcium gradients in pancreatic acinar cells. *J Biol. Chem.* **280** 15794-9.

Dolman N.J. and Tepikin A.V. (2006) Calcium gradients and the Golgi. *Cell Calcium* **40(5-6)** 505-12.

Durr G., Strayl J., Plemper R., Elbs S., Klee S.K., Catty P., Wolf D.H., and Rudolph H.K. (1998) The *medial*-Golgi Ion Pump Pmr1 Supplies the Yeast Secretory Pathway with Ca^{2+} and Mn^{2+} Required for Glycosylation, Sorting, and Endoplasmic Reticulum-Associated Protein Degradation. *Mol Biol Cell.* **9(5)** 1149-62.

Erickson T, Liu L, Gueyikian A, Zhu X, Gibbons J, Williamson PR. (2001) Multiple virulence factors of Cryptococcus neoformans are dependent on VPH1. *Mol Microbiol*. 42:1121-31.

Ernst, JF. (2000) Transcription factors in *Candida albicans* - environmental control of morphogenesis. *Microbiology*. 146:1763-74.

Fearon E.R., and Vogelstein B. (1990) A Genetic Model for Colorectal Tumorigenesis. *Cell* **61** 759-67.

Finnigan GC, Cronan GE, Park HJ, Srinivasan S, Quiocho FA, Stevens TH (2012) Sorting of the yeast vacuolar-type, proton-translocating ATPase enzyme complex (V-

ATPase): identification of a necessary and sufficient Golgi/endosomal retention signal in Stv1p. *J Biol Chem*. 287:19487-500.

Fivaz M. and Meyer T. (2005) Reversible translocation of kRas but not hRas in Hippocampal neurons regulated by calcium/calmodulin. *J. Cell Biol.* **170** 429-41.

Fleet J.C., Eksir F., Hance K.W. and Wood R.J. (2002) Vitamin D-inducible calcium transport and gene expression in three Caco-2 cell lines. *Gastrointestinal and Liver Physiology* **283** G618-G625

Freedman R.A., Weiser M.M., and Isselbacher K.J. (1997) Calcium translocation by Golgi and lateral-basal membrane vesicles from rat intestine: decrease in vitamin D-deficient rats. *Proc Natl Acad Sci USA* **74(8)** 3612-3616.

Fudge N.J., Kovacs C.S. (2010) Pregnancy Up-Regulates Intestinal Calcium Absorption and Skeletal Mineralization Independently of the Vitamin D Receptor. *Endocrinology* **151(3)** 886-95.

Fumarola C., La Monica S., Alfieri R.R., Borra E., and Guidotti G.G. (2005) Cell size reduction induced by inhibition of the mTOR/S6K-signaling pathway protects Jurkat cells from apoptosis. *Cell Death and Differentiation* **12** 1344-57.

Gagliani, N., Hu B., Huber S., Elinav E., and Flavell R.A. (2014) The Fire Within: Microbes Inflame Tumors. *Cell* **157** 776-83.

Galluzzi L., Vitale I., Abrams J.M., Alnemri E.S., Baehrecke E.H., Blagosklonny M.V., Dawson T.M., Dawson V.L., El-Deiry W.S., Fulda S., Gottlieb E., Green D.R.,

Hengartner M.O., Kepp O., Knight R.A., Kumar S., Lipton S.A., Lu X., Madeo F., Malorni W., Mehlen P., Nunez G., Peter M.E., Piacentini M., Rubinsztein D.C., Shi Y., Simon H-U., Vandenabeele P., White E., Yuan J., Zhivotovsky B., Melino G., Kroemer G. (2012) Molecular definitions of cell death subroutines: recommendations of the Nomenclature Committee on Cell Death 2012. *Cell Death and Differentiation* **19** 107-20.

Gamarra S., Rocha E.M., Zhang Y.Q., Park S., Rao R., Perlin D.S. (2010) Mechanism of the synergistic effect of amiodarone and fluconazole in *Candida albicans*. *Antimicrob. Agents Chemother.* **54** 1753-61.

Gasteiger E., Hoogland C., Gattiker A., Duvaud S., Wilkins M.R., Appel R.D., Bairoch A.; Protein Identification and Analysis Tools on the ExPASy Server; (In) John M. Walker (ed): The Proteomics Protocols Handbook, Humana Press (2005). pp. 571-607

Grossmann J., Walther K., Artinger M., Rümmele P., Woenckhaus M., Schölmerich J. (2002) Induction of apoptosis before shedding of human intestinal epithelial cells. *Am J. Gastroenterol.* **97(6)** 1421-8.

Ha K., White T.C. (1999) Effects of Azole Antifungal Drugs on the Transition from Yeast Cells to Hyphae in Susceptible and Resistant Isolates of the Pathogenic Yeast *Candida albicans*. *Antimicrob. Agents Chemother.* **43** 763-8.

Hassan C., Lang G.D., and Rubin D.T. (2011) Epidemiology and Screening of Colorectal Cancer. *Atlas of Virtual Colonoscopy* Chapter 3 pp 55-63 *Fix this book ref.

Hall P.A., Coates P.J., Ansari B., and Hopwood D. (1994) Regulation of cell number in the mammalian gastrointestinal tract: the importance of apoptosis. *Journal of Cell Science* **107(12),** 3569-3577.

Hemenway CS, Dolinski K, Cardenas ME, Hiller MA, Jones EW, Heitman J. (1995) vph6 mutants of Saccharomyces cerevisiae require calcineurin for growth and are defective in vacuolar H(+)-ATPase assembly. *Genetics*. 141:833-44.

Hilty J, Smulian AG, Newman SL. (2008)The *Histoplasma capsulatum* vacuolar ATPase is required for iron homeostasis, intracellular replication in macrophages and virulence in a murine model of histoplasmosis. *Mol. Microbiol*. 70:127-39.

Hirsch D., Barker N., McNeil N., Hu Y., Camps J., McKinnon K., Clevers H., Ried T., Gaiser T. (2013) LGR5 positivity defines stem-like cells in colorectal cancer. *Carcinogenesis* **12(20),** bgt377v2-bgt377.

Housseau F. and Sears C.L. (2010) Enterotoxigenic *Bacteroides fragilis* (ETBF)-mediated colitis in Min (Apc+/-) mice *Cell Cycle* **9(1)** 3-5.

Hu Z., Bonifas J.M., Beech J., Bench G., Shigihara T., Ogawa H., Ikeda S., Mauro T., Epstein E.J. (2000) Mutations in *ATP2C1*, encoding a calcium pump, cause Hailey-Hailey disease. *Nature Genetics* **24** 61-5.

Johnson RM, Allen C, Melman SD, Waller A, Young SM, Sklar LA, Parra KJ. (2010) Identification of inhibitors of vacuolar proton-translocating ATPase pumps in yeast by high-throughput screening flow cytometry. *Anal Biochem*. 398:203-11.

Kane PM. (2007) The long physiological reach of the yeast vacuolar H^+-ATPase. *J Bioenerg Biomembr*. 39:415-21.

Kawasaki-Nishi S, Nishi T, Forgac M. (2001) Yeast V-ATPase complexes containing different isoforms of the 100-kDa a-subunit differ in coupling efficiency and in vivo dissociation. *J Biol Chem*. 276:17941-8.

Krebs, J. and Michalak M. (2007) Calcium: A Matter of Life or Death. Elsevier.

Koh AY, Kohler JR, Coggshall KT, Van Rooijen N, Pier GB. (2008) Mucosal damage and neutropenia are required for *Candida albicans* dissemination. *PLoS Pathogens* 2(4):e35.

Lamprecht S.A. and Lipkin M. (2003) Chemoprevention of colon cancer by calcium, vitamin D and folate: molecular mechanisms. *Nature Reviews Cancer* **3** 601-14.

Lapinskas P.J., Cunningham K.W., Liu X.F., Fink G.R., and Culotta V.C. (1995) Mutations in PMR1 suppress oxidative damage in yeast cells lacking superoxide dismutase. *Mol Cell Biol* **15(3)** 1382-8.

Lappe J.M., Travers-Gustafsonn D., Davies K.M., Recker R.R., and Heaney R.P. (2007) Vitamin D and calcium supplementation reduces cancer risk: results of a randomized trial. *Am J Clin Nutr* **85(6)** 1586-91.

Lavaggi M.L., Cabrera M., Pintos C., Arredondo C., Pachon G., Rodriguez J., Raymondo S., Pacheco J.P., Cascante M., Olea-Azar C., de Cerain A.L., Monge A., Cerecetto H.,

and Gonzalez M. (2011) Novel Phenazine 5,10-Dioxides Release *OH in Simulated Hypoxia and Induce Reduction of Tumour Volume *In Vivo*. ISRN Pharmacol. 314209

Leitch S., Feng M., Muend S., Braiterman L.T., Hubbard A.L. and Rao R. (2011) Vesicular distribution of Secretory Pathway Ca2+-ATPase isoform 1 and a role in manganese detoxification in liver-derived polarized cells. Biometals **24(1)** 159-70.

Loboda A., Nebozhyn M.V., Watters J.W, Buser C.A., Shaw P.M., Huang P.S., Veer L.V., Tollenaar R.AEM., Jackson D.B., Agrawal D., Dai H., Yeatman T.J. (2011) EMT is the dominant program in human colon cancer. *BMC Medical Genomics* **4(9)**

Majno and Joris (1995) Apoptosis, oncosis, and necrosis. An overview of cell death. *Am J Pathol* **146(1)** 3-15.

Manca S., Magrelli A., Cialfi S., Lefort K., Ambra R., Alimandi M., Biolcati G., Uccelletti D., Palleschi C., Screpanti I., Candi E., Melino G., Salvatore M., Taruscio D., and Talora C. (2011) Oxidative stress activation of miR-125b is part of the molecular switch for Hailey-Hailey disease manifestation. *Experimental Dermatology* **20(11)** 932-7.

Manolson MF, Proteau D, Preston RA, Stenbit A, Roberts BT, Hoyt MA, Preuss D, Mulholland J, Botstein D, Jones EW. (1992) The VPH1 gene encodes a 95-kDa integral membrane polypeptide required for in vivo assembly and activity of the yeast vacuolar H(+)-ATPase. *J Biol Chem*. 267:14294-303.

Manolson MF, Wu B, Proteau D, Taillon BE, Roberts BT, Hoyt MA, Jones EW. (1994) STV1 gene encodes functional homologue of 95-kDa yeast vacuolar H(+)-ATPase subunit Vph1p. *J Biol Chem*. 269:14064-74.

McKenzie CGJ, Koser U, Lewis LE, Bain JM, Mora-Montes HM, Barker RN, Gow NAR. Erwig LP. (2010) Contribution of *Candida albicans* cell wall components to recognition by and escape from murine macrophages. *Infect Immun*. 78:1650-8.

Micaroni M. and Malquori L. (2013) Overlapping *ATP2C1* and *ASTE1* Genes in Human Genome: Implications for SPCA1 Expression? *Int J Mol Sci* **14(1)** 674-83.

Michael-Robinson, J.M., Reid L.E., Purdie D.M., Biemer-Huttmann A-E., Walsh M.D., Pandeya N., Simms L.A., Young J.P., Leggett B.A., Jass J.R., and Radford-Smith G.L. (2001) Proliferation, Apoptosis and Survival in High-Level Microsatellite Instability Sporadic Colorectal Cancer. *Clin Cancer Res* **7** 2347-56.

Milgrom E, Diab H, Middleton F, Kane PM. Loss of vacuolar proton-translocating ATPase activity in yeast results in chronic oxidative stress. *J Biol Chem*. 282:7125-36.

Minghui X., Mohamalawari D., and Rao R. (2005) A Novel Isoform of the Secretory Pathway Ca2+/Mn2+-ATPase, hSPCA2, Has Unusual Properties and Is Expressed in the Brain. *Journal of Biological Chemistry* **280** 11608-14.

Murín R., Verleysdonk S., Raeymaekers L., Kaplán P., and Lehotský J. (2006) Distribution of Secretory Pathway Ca2+ ATPase (SPCA1) in Neuronal and Glial Cell Cultures. *Cellular and Molecular Neurobiology* **26(7/8)** 1355-65.

Nelson H, Mandiyan S, Nelson N. (1994) The Saccharomyces cerevisiae VMA7 gene encodes a 14-kDa subunit of the vacuolar H(+)-ATPase catalytic sector. *J Biol Chem*. 269:24150-5.

Neufeld, T. (2012) Autophagy and cell growth – the yin and yang of nutrient responses. *J Cell Sci* **125** 1-10.

Neugut A.I., Marvin M.R., Chabot J.A. (2001) Adenocarcinoma of the small bowel. *Surgical Treatment: Evidence-Based and Problem-Oriented*

Noble SM, French S, Kohn LA, Chen V, Johnson AD. (2010) Systematic screens of a *Candida albicans* homozygous deletion library decouple morphogenetic switching and pathogenicity. *Nat Genet*. 42:590-8.

Noble SM, Johnson AD (2005) Strains and Strategies for Large-Scale Gene Deletion Studies of the Diploid Human Fungal Pathogen *Candida albicans Eukaryotic Cell* 4:298-309

Palmer GE. (2011) Vacuolar trafficking and Candida albicans pathogenesis. Commun Integr Biol. 4:240-242.

Payne S., Gibson G., Wynne A., Hudspith B., Brostoff J., and Tuohy K. (2003) In vitro stuies on colonization resistance of the human gut microbiota to Candida albicans and the effects of tetracycline and Lactiobacillus plantarum LPK. *Curr Issues Intest Microbiol* **4(1)** 1-8.

Perzov N, Padler-Karavani V, Nelson H, Nelson N (2002) Characterization of yeast V-ATPase mutants lacking Vph1p or Stv1p and the effect on endocytosis. *J Exp Biol.* 205:1209-19.

Pestov N.B., Dmitriev R.I., Kostina M.B., Korneenko T.V., Shakhparonov M.I., and Modyanov N.N. (2012) Structural evolution and tissue-specific expression of tetrapod-specific second isoform of secretory pathway Ca^{2+}-ATPase. *Biochemical and Biophysical Research Communications* **417(4)** 1298-1303.

Poltermann S, Nguyen M, Gunther J, Wendland J, Hartl A, Kunkel W, Zipfel PF, Eck R (2005) The putative vacuolar ATPase subunit Vma7p of Candida albicans is involved in vacuole acidification, hyphal development and virulence. *Microbiology* 151:1645-55.

Raines SM, Rane HS, Bernardo SM, Binder JL, Lee SA, Parra KJ. (2013) Deletion of vacuolar proton-translocating ATPase V(o)a isoforms clarifies the role of vacuolar pH as a determinant of virulence-associated traits in *Candida albicans*. *J Biol Chem*. 288:6190-201.

Reed J.C. (2000) Mechanisms of Apoptosis. *Am J Pathol* **157(5)** 1415-30.

Ruemmele F.M., Schwartz S., Seidman E.G., Dionne S., Levy E., Lentze M.J. (2003) Butyrate induced Caco-2 cell apoptosis is mediated via the mitochondrial pathway. **52(1)** 94-100.

Sarker R., Valkhoff V.E., Zachos N.C., Lin R., Cha B., Chen T., Guggino S., Zizak M., de Jonge H., Hogema B., Donowitz M. (2011) NHERF1 and NHERF2 are necessary for

multiple but usually separate aspects of basal and acute regulation of NHE3 activity. *Am J Phyisiol Cell Physiol.* **300(4)** C771-82.

Schulze J, Sonnenborn U. (2009) Yeast in the gut: from commensals to infectious agents. *Dtsch Arztebl Int.* 106:837-42.

Shen J, Guo W, Köhler JR. (2005) CaNAT1, a heterologous dominant selectable marker for transformation of *Candida albicans* and other pathogenic Candida species. *Infect Immun.* 73:1239-42.

Singh, R., Kaushik S., Wanag Y., Xiang Y., Novak I., Komatsu M., Tanaka K., Cuervo A.M., Czaja M.J. (2009) Autophagy regulates lipid metabolism. *Nature* **458** 1131-5.

Steinhauser M.L., Bailey A.P., Senyo S.E., Guillermier C., Perlstein T.S., Gould A.P., Lee R.T., Lechene C.P. (2012) Multi-isotope imaging mass spectrometry quantifies stem cell division and metabolism. *Nature* **481(7382)** 516-9.

Sun D., Lennernas H., Welage L.S., Barnett J.L., Landowski C.P., Foster D., Fleisher D., Lee K.D., Amidon G.L. (2002) Comparison of human duodenum and Caco-2 gene expression profiles for 12,000 gene sequences tags and correlation with permeability of 26 drugs. *Pharm Res.* **19(10)** 1400-16.

Takabe K., Paugh S.W., Milstien S. and Spiegel S. (2008) "Inside-Out" Signaling of Sphingosine-1-Phosphate: Therapeutic Targets. *Pharmacological Reviews* **60(2)** 181-95.

Tanida, I., A. Hasegawa, H. Iida, Y. Ohya and Y. Anraku. (1995). Cooperation of calcineurin and vacuolar H(+)-ATPase in intracellular Ca2+ homeostasis of yeast cells. *J Biol Chem.* 270**:** 10113–10119.

Tarsio M, Zheng H, Smardon AM, Martínez-Muñoz GA, Kane PM. (2011) Consequences of loss of Vph1 protein-containing vacuolar ATPases (V-ATPases) for overall cellular pH homeostasis. *J Biol Chem*. 286:28089-96.

Uhl MA, Johnson AD. (2001) Development of *Streptococcus thermophilus* lacZ as a reporter gene for Candida albicans. *Microbiology*. 147:1189-95.

Van Baelen, K., Dode L., Vanoevelen J., Callewaert G., De Smedt H., Missiaen L., Parys J.B., Raeymaekers L. Wuytack F. (2004) The Ca2+/Mn2+ pumps in the Golgi apparatus. *Biochimica et Biophysica Acta* **1742** 103-12.

Vylkova S, Carman AJ, Danhof HA, Collette JR, Zhou H, Lorenz MC. (2011) The fungal pathogen *Candida albicans* autoinduces hyphal morphogenesis by raising extracellular pH. *MBio* 2:e00055-11.

Wei Y., Marchi V., Wang R., and Rao R. (1999) An N-Terminal EF Hand-like Motif Modulates Ion Transport by Pmr1, the Yeast Golgi Ca2+/Mn2-ATPase. *Biochemistry* **38(44)** 14534-41.

Wootton L.L., Argent C.C.H., Wheatley M. and Michelangeli F. (2004) The expression, activity and localization of the secretory pathway Ca2+-ATPase (SPCA1) in different mammalian tissues. *Biochimica et Biophysica Acta- Biomembranes* **1664(2)** 189-97.

Zhang YQ, Gamarra S, Garcia-Effron G, Park S, Perlin DS, Rao R. (2010) Requirement for ergosterol in V-ATPase function underlies antifungal activity of azole drugs. *PLoS Pathog*. 6(6):e1000939.

Zhang YQ, Rao R. (2010) Beyond ergosterol: linking pH to antifungal mechanisms. *Virulence*. **1**:551-4.

Zhang Y, Rao R. (2012) The V-ATPase as a target for antifungal drugs. *Curr Protein Pept Sci* 12:134-40.

Name: Cassandra A. Patenaude

Education:

2009 - 2014	PhD	Physiology, BCMB	Johns Hopkins School of Medicine
2007	BS	Biochemistry; Molecular and Cellular Biology Minor: Chemistry	University of Maine, Orono

Research Experience

Sept 2009 – Sept 2014 Graduate Student — Johns Hopkins School of Medicine
BCMB Graduate Program
Baltimore, MD

- Studied growth defects in colon cancer cell lines induced by hairpin RNA against the secretory pathway Ca^{2+}/Mn^{2+} ATPases.
- Examined the role of V-ATPase isoforms in *C. albicans* in the context of infection establishment and invasive growth phenotype.

Aug 2007 – 2009 Research Technician — Boston University School of Medicine
Department of Biochemistry
Boston, MA

- Identified key factors involved in aortic carboxypeptidase-like protein (ACLP) transcription and found culture conditions that induce ACLP expression.
- Investigated ACLP expression in non-smooth muscle cell type and found increased ACLP levels following tissue growth in vivo.
- Studied binding interactions of ATF2 at Csrp2 gene promoter in collaboration with Dr. Yet (National Health and Research Institutes, Taiwan).

Sept – Dec 2006 Student Research Assistant — University of Maine
Department of Biochemistry, Orono, ME

- Analyzed a set of activated retroelements in zebrafish five hours post-fertilization to serve as monitors of epigenetic silencing during development.
- Proposed origins of transcripts within the genome and specified likely elements responsible for activity.

June – Aug 2005 Summer Research Intern — University of Massachusetts
Department of Biology, Boston, MA
Research Experience for Undergraduates National Science Foundation.

- Determined the sub-cellular localization of a sporulation-specific protein, Spo71, in live yeast.
- Participated in generating epitope-tagged mutant lines to be used for further characterization.

Sept 2003 – May 2005 | Laboratory Aid | University of Maine, Department of Biochemistry, Orono, ME

- Assessed combined toxicity of heavy metals and lipopolysaccharides in wild caught killifish liver and gill tissues.
- Evaluated biological impact of xenoestrogen exposure in fishes to assess varying sewage treatment protocol.

Committee Assignments:

Johns Hopkins School of Medicine, Department of Physiology

2012- 13 | Co-chair | Physiology Friday Research Series

Boston University School of Medicine

2008 – 09 | Floor Representative | Biochemistry Sustainability Committee

Memberships and Activities

Teaching

Sept 2013– Dec 2013 | Tutor | Johns Hopkins School of Medicine, BCMB Program

- Served as tutor for a core course, Molecular Biology and Genomics.

Sept 2004– Sept 2005 | Peer Tutor | University of Maine, Department of Chemistry

- Led weekly group learning projects to stimulate interest and improve performance in chemistry in first year college students.

Presentations

2012 FASEB Science Research Conference: Transport ATPases: From Molecules to Maladies
Base Village, Snowmass Village, CO
Patenaude CA, Zhang, YQ, Rao R
"Isoform Specific Roles of V-ATPase subunit *a* in *C. albicans* pathogenicity" (Poster presentation)

2005 40th Annual National Collegiate Honors Council Conference
St. Louis, MO
Patenaude CA, Notch EG, Miniutti DM, Mayer GD
"The Combined Effects of Cyanobacterial Lipopolysaccharides and Heavy Metals" (Poster presentation)

2005 Biology Department
University of Massachusetts, Boston, MA
Patenaude CA, Baker C, Huang L
"Epitope Tagging of a Sporulation Specific Protein, Spo71p"
(Poster presentation)

Bibliography

Original Articles

1. **Patenaude C**, Zhang Y, Cormack B, Kohler J, Rao R. Essential Role for Vacuolar Acidification in *Candida albicans* Virulence. J Biol Chem. 2013:288(36):26256-64.

2. Luchsinger LL, **Patenaude CA**, Smith BD, Layne MD. Myocardin-related Transcription Factor-A Complexes Activate Type I Collagen Expression in Lung Fibroblasts. J Biol Chem. 2011;286(51):44116-25. PMCID: PMC3243519

3. Lin D-W, Chang I-C, Tseng A, Wu M-L, Chen C-H, **Patenaude CA**, Layne MD, Yet S-F. Transforming Growth Factor β Up-regulates Cysteine-rich Protein 2 in Vascular Smooth Muscle Cells via Activating Transcription Factor 2. J Biol Chem. 2008;283(22):15003-14. PMCID: PMC2397482

Non-Peer Reviewed Articles

1. Notch EG, **Patenaude CA**, Miniutti DM, Hicks AN, and Mayer GD. "Effect of lipopolysaccharides from Microcystis and Lyngbya on metal toxicity in Fundulus heteroclitus." MDIBL Bull, 2005;44:126-127.

2. Mayer GD, Berry JP, **Patenaude CA**, and Walsh PJ. "Effect of lipopolysaccharides from Microcystis and Lyngbya on metal toxicity in Fundulus heteroclitus." Bull. of the MDIBL, 2004;43:143-144.

Rajini Rao	Mark Donowitz
Director, Cellular and Molecular Medicine	Director, Basic Research GI Division
Co-advisor	Co-advisor
[Faculty Sponsor and reader]	[Reader]